Activation of methane by size-selected iron cluster cations, Fe_n^+ ($n=2-15$): Cluster-CH_x ($x=0-3$) bond energies and reaction mechanisms

Rohana Liyanage, Xiao-Guang Zhang, and P. B. Armentrout
Department of Chemistry, University of Utah, Salt Lake City, Utah 84112

(Received 17 May 2001; accepted 6 September 2001)

The kinetic energy dependences of the reactions of Fe_n^+ ($n=2-15$) with CD_4 are studied in a guided ion beam tandem mass spectrometer over the energy range of 0–10 eV. All reactions exhibit thresholds and two main products, Fe_nD^+ and $Fe_nCD_2^+$, are formed. These primary products decompose at higher energies to form secondary and higher order products, Fe_nCD^+, Fe_nC^+, $Fe_{n-1}D^+$, $Fe_{n-1}CD_2^+$, $Fe_{n-1}CD^+$, and $Fe_{n-1}C^+$. The cross-section magnitudes for the dehydrogenation products, $Fe_nCD_2^+$, are observed to vary considerably as a function of cluster size; subsequent dehydrogenation to form Fe_nC^+ becomes more facile for larger clusters. Thresholds for the various primary and secondary reactions are analyzed and bond energies for iron cluster cation bonds to C, CD, CD_2, and CD_3 are determined. As a function of cluster size, these bond energies rapidly reach relatively constant values, which are argued to lie close to bulk phase values. The relative magnitudes in these bond energies are consistent with simple bond order considerations. On the basis of this thermochemistry, we find that there are barriers to the primary dehydrogenation reactions for all the clusters, except $n=3$ and 4. Evidence that this barrier for $n\geqslant 5$ corresponds to the chemisorption step is discussed. © *2001 American Institute of Physics.*
[DOI: 10.1063/1.1413983]

I. INTRODUCTION

Catalytic reactions of CH_4 with transition metal surfaces are of considerable importance in many industrial processes. Decreasing resources of crude oil may cause a shift to coal and natural gas as the feedstock for chemical industry and transportation fuels market. These resources can be converted into CO and H_2 by partial oxidation or steam reforming processes, which subsequently can be converted to hydrocarbons in the Fischer–Tropsch (FT) process[1] on precipitated iron catalysts. In the processes for the steam reforming of natural gas over nickel and iron catalysts,[2] it is thought that the rate limiting step in the reaction of $CH_4+H_2O\rightarrow CO+3H_2$ is the dissociation of methane. Iron and nickel are believed to be good catalysts, as they reduce the C–H bond activation energy to about 33–84 kJ/mol depending on the Ni/Fe mixture.[3] The FT process synthesizes linear and branched hydrocarbons and oxygenated products. The fuels produced with FT synthesis are normally of good purity and are environmentally clean in comparison to conventional crude oil-derived fuels because of low aromaticity and zero sulfur content. Intermediates believed to be important in FT processes on iron catalysts include $(Fe_s)-H$, $(Fe_s)-C$, $(Fe_s)-CH$, $(Fe_s)-CH_2$, and $(Fe_s)-CH_3$,[1] where the subscript s refers to surface atoms.

Iron carbide is a new material employed in steelmaking[4] and intended to replace conventional direct reduced iron (DRI). In conventional DRI, the maximum stoichiometric carbon content reaches only 3.5% and a small carbidic outer layer is formed, whereas in iron carbide, more than 95% can be carbide. Stelling invented the first process for production of iron carbide from iron ores, but this was not successfully implemented on an industrial scale.[5] In this method, iron is carburized using CO, while more recent methods use mainly CH_4 as the reducing and carburizing gas. Depending on the precursor material (Fe or Fe_2O_3), the reducing gas, and the carburizing gas,[6,7] the solid product obtained can be bulk Fe_2C, Fe_3C, or Fe_5C_2.

There is little fundamental experimental work investigating the activation of methane on iron surfaces. Wright and co-workers[8] investigated the adsorption of methane and ethane on evaporated metal films. They found that the chemisorption of methane on iron films occurs at 170 °C, indicating that this is an activated process, but no activation energies could be derived. Anderson has calculated methane activation energies of 32, 27, and 126 kJ/mol, respectively, on Fe(100), Fe/Fe(100), and Fe(110) surfaces.[9] Anderson also calculated binding energies between methane fragments and iron dimers and estimated the dehydrogenation energies for each fragment.[10]

Studies of clusters of transition metal elements are of interest because of their potential as models for surface reactions and heterogeneous catalysis. The size dependence of the reactivities of the transition metal clusters is a fascinating and intriguing issue in modern cluster chemistry and has attracted much attention in both theoretical and experimental fields. Experimentally, the guided ion beam technique has proven to be successful in providing kinetic energy-dependent reaction cross sections which can be interpreted to yield accurate bond energies for metal–ligand complexes[11] and cluster-ligand complexes.[12–20] In the present study, we use guided ion beam tandem mass spectrometry to investi-

gate the reactions of size-selected iron cluster cations (2–15 atoms) with methane. By examining the kinetic energy dependence of these reactions, we are able to determine energetics for a number of processes analogous to those relevant in FT synthesis and related chemistries. The goal of this study is to give insight into C–H bond activation on iron surfaces and to provide quantitative thermodynamic information regarding the intermediates and products formed in these reactions. This thermodynamic information is compared to available theoretical estimates and used as a probe of the electronic structure of the bare iron clusters. Significantly, this work provides bond energies for hydrocarbon fragments, CH, CH_2, and CH_3, to size-specific iron cluster cations. Analogous experimental information is unavailable for surfaces and clusters of any metal.

II. EXPERIMENT

The ion beam apparatus and experimental techniques used in this work have been described in detail elsewhere,[21] so only a brief description is given here. Iron cluster cations are formed in a laser vaporization/supersonic expansion source.[22] The output of an Oxford ACL 35 copper vapor laser operating at 8 kHz is tightly focused onto a continuously translating and rotating iron target rod (cold-rolled steel) inside an aluminum source block. The optimum pulse energy for iron cluster ion production ranges between 3–4 mJ/pulse. The vaporized material is entrained in a continuous flow ($5-6\times10^3$ sccm) of He passing over the ablation surface. Frequent collisions and rapid mixing lead to the formation of thermalized clusters as they travel down a 2 mm diameter ×63 mm long condensation tube. Although direct measurements of the internal temperatures of the clusters are not possible, previous studies have indicated that the clusters are not internally excited and likely to be near room temperature.[23–25]

This seeded helium flow then undergoes a mild supersonic expansion in a field-free region and is skimmed. Positively charged ions are accelerated, focused, and injected into a 60° magnetic sector momentum analyzer. The mass selected ions are decelerated and focused into a rf octopole ion guide[26] that extends through a reaction cell. The octopole guide is biased with dc and rf voltages. The former allows us to accurately control the translational energy of the incoming ions while the latter establishes a radial potential that efficiently traps the parent and product ions that travel through the octopole. The pressure of CD_4 neutral reactant gas (99.8% purity) in the reaction cell is kept relatively low to reduce the probability of multiple collisions with the ions. To test this, all studies were conducted at two pressures of CD_4, ~0.2 and ~0.4 mTorr. The product and remaining reactant ions drift to the end of the octopole, where they are extracted and injected into a quadrupole mass filter for mass analysis. Ion intensities are measured with a Daly detector[27] coupled with standard pulse counting techniques. Reactant ion intensities used in these studies ranged from $0.5-1.0\times10^6$ ions/s. Observed product intensities are converted to absolute reaction cross sections, as discussed in detail elsewhere.[28] Absolute errors in the cross sections are on the order of ±30%.

Results for each reaction system were repeated several times to ensure their reproducibility. CID experiments with Xe were performed on all the cluster ions to verify their identity and the absence of any excessive internal excitation. In all instances, CID thresholds are consistent with those previously reported.[25] The absolute zero in the kinetic energy of the ions and their energy distributions (the latter varying with cluster size from 0.7–2 eV) were measured using the octopole as a retarding energy analyzer. The error associated with the absolute energy scale is 0.05 eV in the lab frame. Kinetic energies in the laboratory frame are converted to center-of-mass (CM) energies using the stationary target approximation, $E(\mathrm{CM})=E(\mathrm{lab})m/(m+M)$, where m and M are the masses of the neutral and ionic reactants, respectively.[28]

Products observed in this work include Fe_nD^+ and $Fe_nCD_x^+$ species, where $x=0-4$. Accurate measurements of the intensities of these species depend on our ability to resolve and transport them efficiently to the detector. Resolving the high intensity Fe_n^+ reactant ions from the low intensity Fe_nD^+ product ions proved to be difficult even when the quadrupole mass analyzer is set to operate at high resolution. In principle, the resolution could be increased sufficiently to separate the parent and product ions, but as this limit is approached, the transmission of the ions is reduced to the extent that the experiments become impractical and inaccurate. Therefore, the experiments are conducted using deuterated methane (to maximize the resolution) and by adjusting the resolution of the quadrupole mass filter to be as high as possible without reducing the product ion intensities. Mass overlap of product ions differing by 2 mass units is easily identified when the energy dependence of their cross sections differ, which is typically the case in this work. However, for the larger clusters, it was difficult to distinguish secondary products such as $Fe_{n-1}CD^+$ and $Fe_{n-1}CD_2^+$. In order to overcome this difficulty, we carefully check the mass overlap associated with differences of 2 mass units, knowing that the lightest possible product in this series is $Fe_{n-1}C^+$. In all cases, the cross sections reported below have been corrected for mass overlap with other species.

III. RESULTS

Iron clusters ranging in size from dimers to 15mers were allowed to react with deuterated methane while varying the relative kinetic energy over a range of thermal to about 10 eV. A complete set of results can be obtained from Ref. 29 and selected clusters are shown below. To help organize the results of the myriad reactions observed, we first note which processes are possible and observed in at least one of the cluster systems. These can be grouped into reactions in which no loss of iron atoms occurs, processes (1)–(4)

$$Fe_n^+ + CD_4 \rightarrow Fe_nD^+ + CD_3, \quad (1)$$

$$\rightarrow Fe_nC^+ + 2D_2, \quad (2)$$

$$\rightarrow Fe_nCD^+ + D + D_2, \quad (3)$$

$$\rightarrow Fe_nCD_2^+ + D_2. \quad (4)$$

At higher energies, products with fewer iron atoms are formed in the simple collision-induced dissociation, reaction (5), and in dissociations of the products formed in reactions (1)–(4). Reactions (6)–(10) comprise the latter types of processes observed

$$Fe_n^+ + CD_4 \rightarrow Fe_{n-1}^+ + Fe + CD_4, \quad (5)$$

$$\rightarrow Fe_{n-1}D^+ + FeCD_3, \quad (6a)$$

$$\rightarrow Fe_{n-1}D^+ + Fe + CD_3, \quad (6b)$$

$$\rightarrow Fe_{n-1}C^+ + Fe + 2D_2, \quad (7)$$

$$\rightarrow Fe_{n-1}CD^+ + Fe + D + D_2, \quad (8)$$

$$\rightarrow Fe_{n-1}CD_2^+ + Fe + D_2, \quad (9)$$

$$\rightarrow Fe_{n-1}CD_3^+ + FeD. \quad (10)$$

A. $Fe^+ + CD_4$

Before examining the results obtained in this study, it is useful to review previous results for the electronic state-specific reactions of atomic iron ions ($n=1$) with methane.[30,31] There, reactions (1) and (4) are observed along with reaction (11)

$$Fe^+ + CD_4 \rightarrow FeCD_3^+ + D. \quad (11)$$

Reaction (1) is the dominant process at all energies. The FeD^+ and $FeCD_3^+$ products are formed beginning at their thermodynamic thresholds, which are similar and about 2.1 eV for reaction of $Fe^+(^4F)$, the first excited state lying 0.23 eV above the ^6D ground state. Although reaction (4) is the least endothermic of all possible reactions, formation of $FeCD_2^+$ requires surmounting a barrier of 0.42 ± 0.06 eV in excess of the endothermicity of 1.03 ± 0.05 eV for reaction of $Fe^+(^4F)$.[31] State-specific results for reaction of ground-state $Fe^+(^6D)$ and excited-state $Fe^+(^4F)$ show that the latter state is much more reactive (by over a factor of 20) for formation of all three product channels. The magnitudes of the reactions of all cluster ions resemble those observed for $Fe^+(^4F)$.

B. Fe_2^+ and $Fe_3^+ + CD_4$

Figure 1 shows results for reaction of the iron dimer cation with methane. Reactions (1)–(6) and (8)–(10) are all observed. It seems likely that the failure to see FeC^+, reaction (7), is simply because its intensity is too small. The dominant process at all energies is hydride formation, reaction (1). At higher energies, this species can lose an iron atom to form FeD^+ in reaction (6). Formation of $Fe_2CD_2^+$ in reaction (4) is also a fairly low energy process, having an apparent threshold about 0.4 eV higher than that observed for $Fe^+(^4F)$. This product can dissociate by iron atom loss to form $FeCD_2^+$ in reaction (9), by further dehydrogenation to form Fe_2C^+ in reaction (2), and by deuterium atom loss to yield Fe_2CD^+ in reaction (3). The former is the dominant dissociation pathway, while the latter two channels show some competition with one another as the cross-section magnitude for Fe_2C^+ decreases when the Fe_2CD^+ product appears. This competition is consistent with dehydrogenation of $Fe_2CD_2^+$ being lower in energy but kinetically less favorable than the D atom loss channel. Fe_2CD^+ can also decompose further by iron atom loss, reaction (8), to form $FeCD^+$, a product that may also be formed by D atom loss from $FeCD_2^+$. The sum of the $FeCD_2^+$ and $FeCD^+$ product cross sections varies smoothly with energy, suggesting that the $FeCD_2^+$ cross section declines because of $FeCD^+$ production, i.e., the latter mechanism. The other two products formed at high energies, Fe^+ and $FeCD_3^+$, are the result of the CID reaction (5) and reaction (10), respectively. The latter process is interesting as it involves formation of a neutral FeD product, which cannot be detected directly. Rather, this assignment is based on the measured threshold for this process, as discussed in detail below.

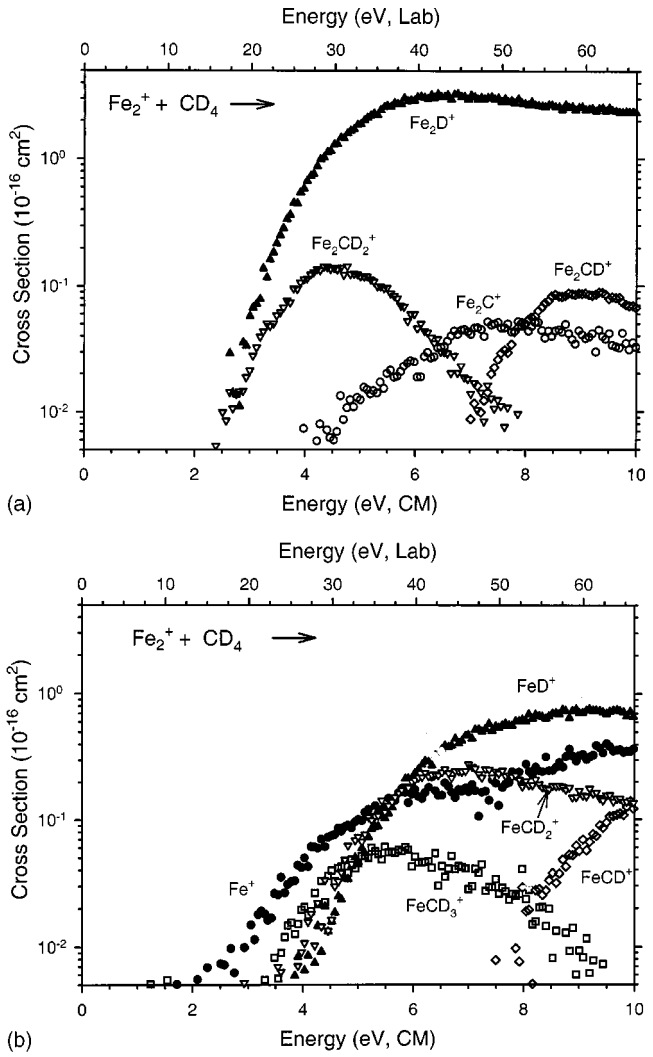

FIG. 1. Product cross sections for the reaction of Fe_2^+ with CD_4 as a function of collision energy in the center of mass (lower x axis) and laboratory frame (upper x axis). Parts (a) and (b) show Fe_2L^+ and FeL^+ cross sections, respectively.

Figure 2 shows results for reaction of the iron trimer cation with methane, where reactions (1)–(10) are all observed. The total reactivity is similar to that of the dimer; however, the CID process is much more important here, consistent with the fact that the iron trimer cation has the weakest bond energy of all iron cluster cations.[25] Also, the lowest energy reaction of the trimer is the dehydrogenation process

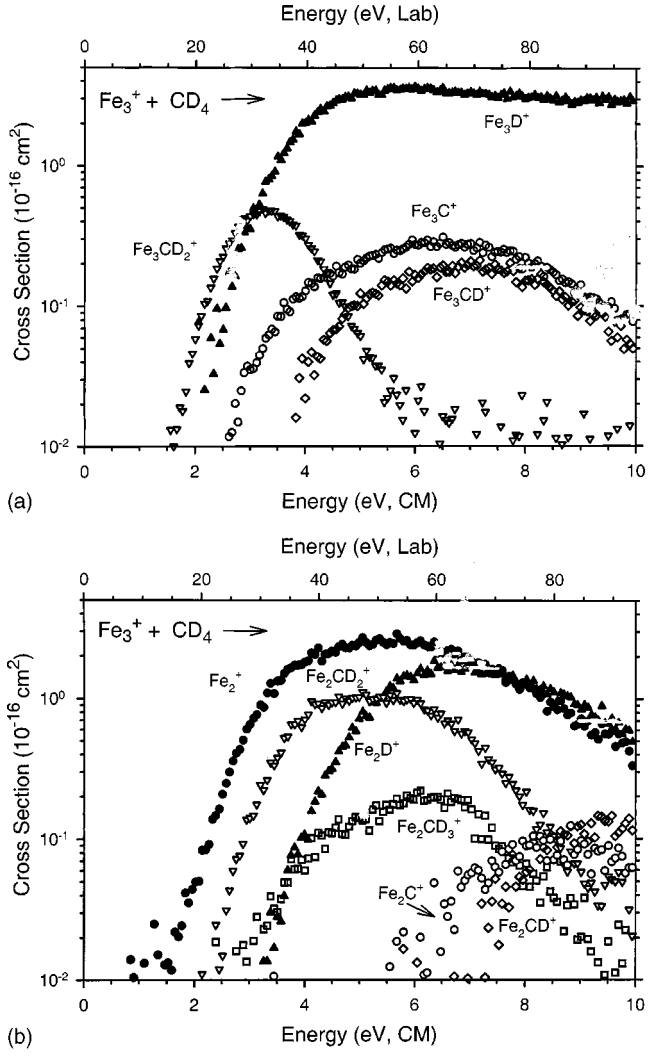

FIG. 2. Product cross sections for the reaction of Fe_3^+ with CD_4 as a function of collision energy in the center of mass (lower x axis) and laboratory frame (upper x axis). Parts (a) and (b) show Fe_3L^+ and Fe_2L^+ cross sections, respectively.

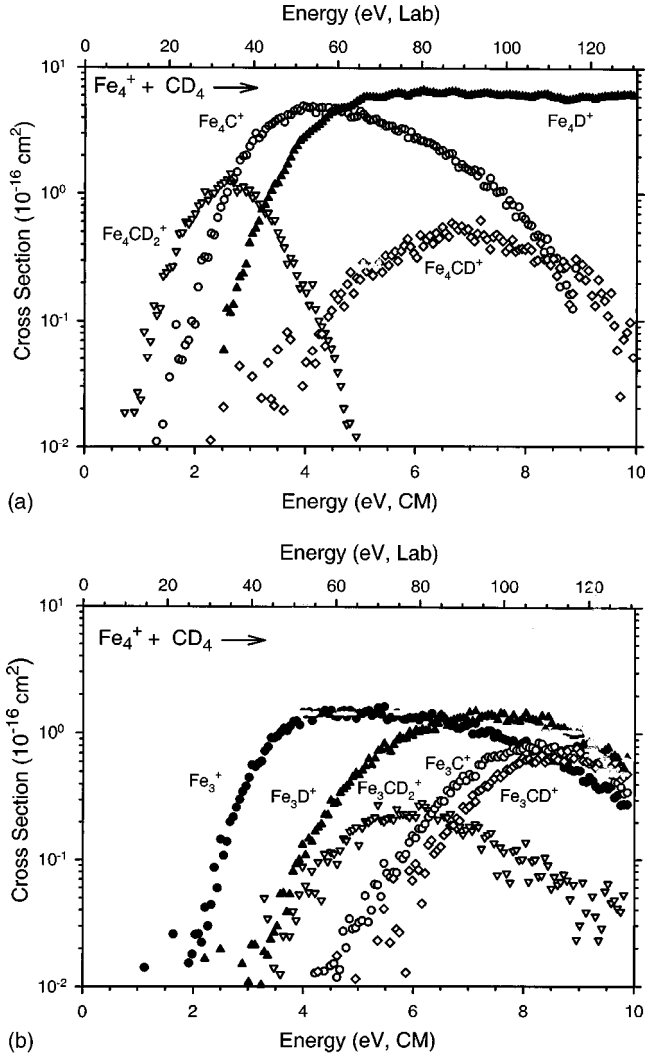

FIG. 3. Product cross sections for the reaction of Fe_4^+ with CD_4 as a function of collision energy in the center of mass (lower x axis) and laboratory frame (upper x axis). Parts (a) and (b) show Fe_4L^+ and Fe_3L^+ cross sections, respectively.

(4), which has an apparent threshold about 1 eV lower than dehydrogenation by the dimer. This cross section reaches a sharp maximum at the energy where the $Fe_3CD_2^+$ product can lose an iron atom to form $Fe_2CD_2^+$. Additional decomposition pathways for this ion include dehydrogenation to form Fe_3C^+ and D atom loss to form Fe_3CD^+. The magnitude of these three decomposition channels nearly accounts for the $Fe_3CD_2^+$ decrease, but there is break in the sum of these four cross sections at about 3 eV. The only channel large enough to account for this behavior is the Fe_3D^+ channel. This indicates that the primary products, $Fe_3CD_2^+$ and Fe_3D^+, compete with each other, which suggests that they share a common precursor, as discussed further below. As for the dimer, the primary Fe_3D^+ and $Fe_3CD_x^+$ products decompose to yield Fe_2D^+ and $Fe_2CD_x^+$ products, reactions (6b)–(9). Possible pathways for Fe_2CD^+ and Fe_2C^+ production involve loss of an iron atom from the Fe_3CD^+ and Fe_3C^+ products, respectively, or loss of D and D_2, respectively, from $Fe_2CD_2^+$. Because the $Fe_2CD_2^+$ cross section falls as the Fe_2CD^+ and Fe_2C^+ cross sections increase, the latter mechanism appears to be the dominant pathway. Formation of $Fe_2CD_3^+$ is observed with a threshold that corresponds to production of a FeD neutral in reaction (10); see below.

C. Fe_4^+ and Fe_5^++CD_4

Reaction cross sections for the iron tetramer cation are shown in Fig. 3. Results for reaction of the iron pentamer cation with methane are very similar. Both clusters undergo reactions (1)–(9), but unlike the smaller clusters, no methylated clusters are observed. As with the trimer, the dehydrogenation reaction (4) is the lowest energy process for the tetramer, with a threshold shifted to lower energies and a resultant increase in magnitude. For the pentamer, this reaction cross section has a higher threshold and smaller magnitude (0.4 $Å^2$ maximum) than that for the tetramer. In contrast to the dimer and trimer systems, however, the $Fe_nCD_2^+$, n = 4 and 5, primary products decompose primarily by further dehydrogenation to form Fe_nC^+ in reaction (2). Loss of Fe and D atoms, reactions (9) and (3), still occurs, but the former is much less important. The double dehydrogenation

reaction is sufficiently facile in these systems that Fe_nC^+ is the dominant product over a 1–2 eV range. Although this product can decompose by iron atom loss to form $Fe_{n-1}C^+$, the magnitude of the $Fe_{n-1}C^+$ cross section cannot account for the decline in the Fe_nC^+ cross section in either system. The only product having a large enough cross section to account for this behavior is Fe_nD^+. This indicates that the primary products, Fe_nD^+ and $Fe_nCD_2^+$, must compete with one another and suggests a common intermediate, as discussed below. The Fe_nD^+ product can decompose by loss of an iron atom; however, this reaction cross section is sufficiently small that it does not alter the magnitude of the primary product cross section over the energy range studied. The $Fe_{n-1}CD^+$ and $Fe_{n-1}C^+$ species can be formed by Fe atom loss from Fe_nCD^+ and Fe_nC^+ products, respectively, or by D and D_2 loss from $Fe_{n-1}CD_2^+$. As for the smaller clusters, the increases in the $Fe_{n-1}CD^+$ and $Fe_{n-1}C^+$ cross sections are accompanied by a commensurate decline in the $Fe_{n-1}CD_2^+$ product cross section and the total cross section for these three product ions varies smoothly with energy. This suggests that the latter mechanism is dominant.

D. $Fe_6^+ + CD_4$

Figure 4 shows results for reaction of the iron hexamer cation with deuterated methane. A striking feature of these results is the virtual absence of the dehydrogenation product, $Fe_6CD_2^+$. However, this species must be formed transiently as double dehydrogenation, reaction (2), is efficient and reaction (3) almost certainly occurs via this primary product as well. Further, $Fe_5CD_2^+$ is also observed, and is likely to be formed by Fe atom loss from $Fe_6CD_2^+$. As for the tetramer and pentamer systems, the Fe_6C^+ product declines because of competition with Fe_6D^+ formation, as no other product has a cross section with sufficient magnitude to account for the decline. Reactions (5)–(9) are all observed with reasonable cross sections. As observed for reactions of smaller clusters, the $Fe_5CD_2^+$ product rapidly dehydrogenates to yield Fe_5C^+ in reaction (7) and lose a D atom to form Fe_5CD^+ in reaction (8). Fe atom loss from Fe_6C^+ and Fe_6CD^+ may also contribute to these cross sections. Again, we find that the total cross section of the three $Fe_5CD_x^+$ ($x=0-2$) products varies smoothly with energy, indicating that the former mechanism dominates.

E. Fe_n^+ ($n=7-9$) + CD_4

Figure 5 shows the reaction cross sections for the iron heptamer cation and methane. Results for the reaction of Fe_8^+ and Fe_9^+ with methane are very similar. Reactions (1)–(9) are observed. In contrast to the hexamer, the dehydrogenation product, $Fe_nCD_2^+$, is again observed with a magnitude that increases by about a factor of 5 from $n=7-9$. The magnitudes of the Fe_nC^+ cross sections increase commensurately. The apparent thresholds for both products shift to lower energies as the cluster size increases. Similar to the reactions of smaller clusters, the Fe_nC^+ cross section declines largely because of competition with Fe_nD^+ formation. Loss of Fe from $Fe_nCD_2^+$ to form $Fe_{n-1}CD_2^+$ is appreciable. Again, the energy dependence of the total cross section of the three

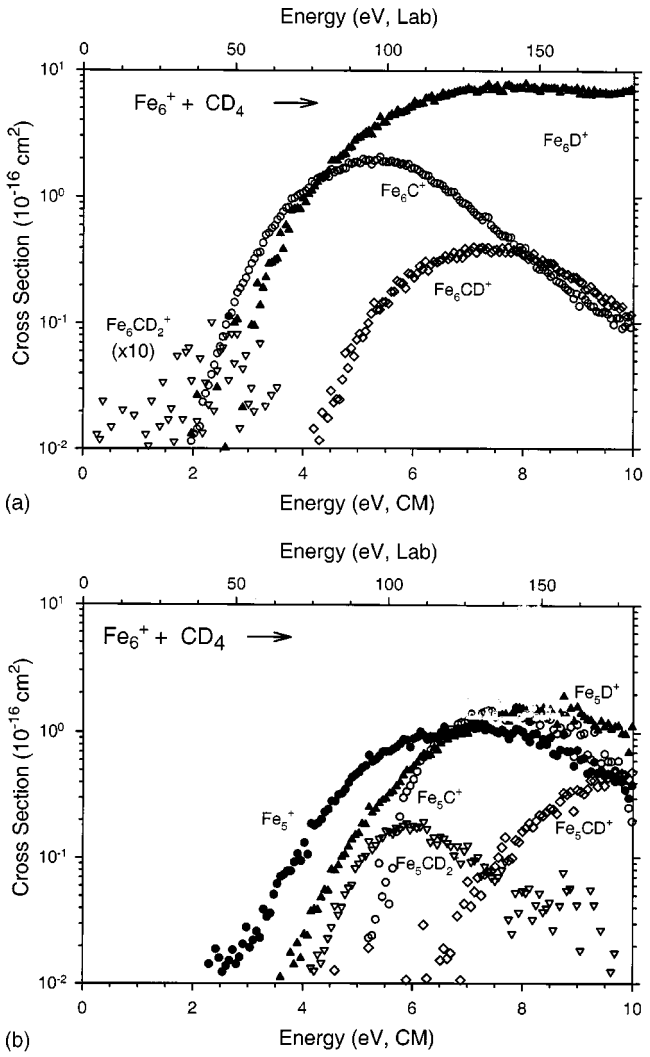

FIG. 4. Product cross sections for the reaction of Fe_6^+ with CD_4 as a function of collision energy in the center of mass (lower x axis) and laboratory frame (upper x axis). Parts (a) and (b) show Fe_6L^+ and Fe_5L^+ cross sections, respectively.

$Fe_{n-1}CD_x^+$ ($x=0-2$) products suggests that the $Fe_{n-1}CD^+$ and $Fe_{n-1}C^+$ products are formed primarily by D and D_2 loss from the $Fe_{n-1}CD_2^+$ product.

F. Fe_n^+ ($n=10-15$) + CD_4

Figure 6 shows results for reactions of the iron 12mer cation with methane, which are representative of the $n=10-15$ mers. Reactions (1)–(9) are observed in all cases, although the quality of the data for reactions (5)–(9) was poor for the largest clusters. One systematic difference in the results for these larger clusters is a gradual decline in the maximum magnitude in the $Fe_nCD_2^+$ cross section as the cluster size increases, from 2.5 Å^2 for $n=10$ to about 0.15 Å^2 for $n=14$ and 15. We find no significant decline in the Fe_nCD^+ at higher energies, which suggests that $Fe_{n-1}CD^+$ is produced by loss of D from $Fe_{n-1}CD_2^+$ rather than loss of an iron atom from Fe_nCD^+. As for the smaller clusters, this conclusion is consistent with a sum of the $Fe_{n-1}CD_2^+$, $Fe_{n-1}CD^+$, and $Fe_{n-1}C^+$ cross sections that smoothly varies with energy.

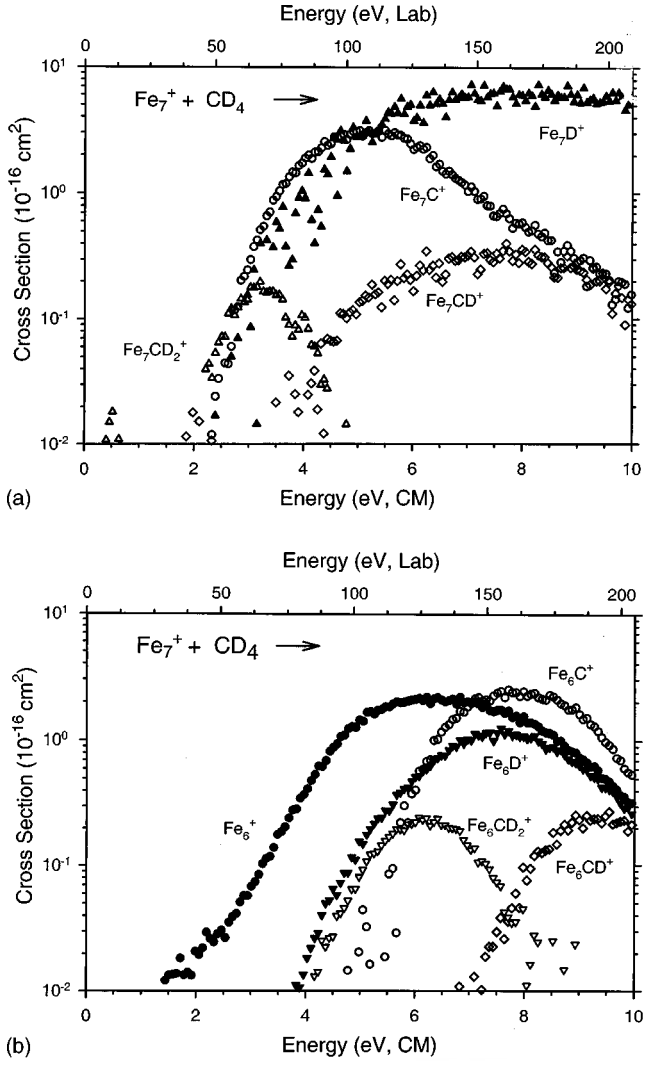

FIG. 5. Product cross sections for the reaction of Fe_7^+ with CD_4 as a function of collision energy in the center of mass (lower x axis) and laboratory frame (upper x axis). Parts (a) and (b) show Fe_7L^+ and Fe_6L^+ cross sections, respectively.

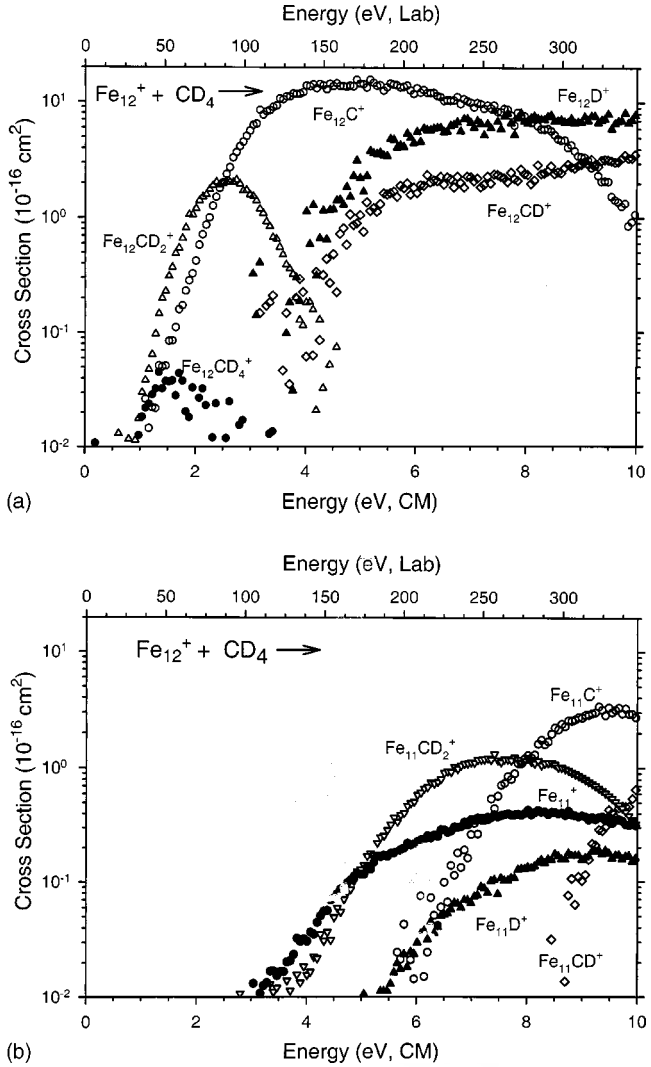

FIG. 6. Product cross sections for the reaction of Fe_{12}^+ with CD_4 as a function of collision energy in the center of mass (lower x axis) and laboratory frame (upper x axis). Parts (a) and (b) show $Fe_{12}L^+$ and $Fe_{11}L^+$ cross sections, respectively.

The most striking result for these clusters is the observation of an adduct, process (12)

$$Fe_n^+ + CD_4 \rightarrow Fe_nCD_4^+ . \quad (12)$$

We verified that this product was not the result of collisional stabilization by checking the dependence of the cross sections on CD_4 pressure. Thus, these species have a lifetime in excess of the experimental time of flight between the collision cell and the detector, about 10^{-4} s. We find that the apparent threshold for formation of $Fe_nCD_4^+$ matches that of the $Fe_nCD_2^+ + D_2$ product channel in all cases.

IV. THRESHOLD ANALYSIS AND THERMOCHEMISTRY

A. Data analysis

The energy dependences of cross sections for endothermic processes in the threshold region are modeled using Eq. (13)

$$\sigma(E) = \sigma_0 \sum g_i (E + E_i - E_0)^N / E, \quad (13)$$

where σ_0 is an energy independent scaling parameter, N is an adjustable parameter, E is the relative kinetic energy, and E_0 is the threshold for reaction at 0 K. The summation is over the rovibrational states of the clusters having energies E_i and populations g_i where $\Sigma g_i = 1$. Vibrational frequencies for the bare metal clusters are obtained as outlined by Loh *et al.*,[21] who used a Debye model suggested by Jarrold and Bower.[32] Before comparison with the data, this model cross section is also convoluted with the kinetic energy distributions of the ion and neutral reactants.[33]

For metal clusters, it has been shown that lifetime effects become increasingly important as the size of the cluster increases.[25] This is because metal clusters have many low frequency vibrational modes such that the lifetime of the transient intermediate can exceed the experimental time available for reaction (approximately 10^{-4} s in our apparatus). Thus, an important component of the modeling of these reactions is to include the lifetime of the reaction, as estimated using statistical Rice–Ramsperger–Kassel–Marcus (RRKM) theory.[34–36] The means to do this has been dis-

TABLE I. Vibrational frequencies for energized molecules (EM) and transition states (TS).

Species	ω_e (cm^{-1})[a]
D–Fe_n^+–CD_3 EM, TTS	(950,870,725),[b] [2157,457,2381(2),1026(2)],[c] 480,[d] 440,[e] 366,[e] 540(3)[d]
D—D | | Fe_n^+–CD_2 TTS	(475,435,363),[e] [585,614,768,944,946,958,963,1367,1403, 2259(2)][f]
D—D | | Fe_n^+–C TTS	(475,435,363),[e] (585,614,768,944)[f]
$Fe_nCD_2^+$ EM	(2134,2201,347,575,550,503),[g] (439,419)[e]
Fe_nCD^+ EM	(648,503),[g] (593,494,419),[e] 2100[h]
Fe_nC^+ EM	(750,686,550)[e]
Fe_nD^+ EM	(950,870,725)[b]

[a]In all cases, species also include $3n-6$ frequencies for the iron cluster calculated as described in Refs. 21 and 32. Degeneracies in parentheses.
[b]Reference 13, TTS removes 950 cm^{-1} frequency from this set.
[c]CD_3 frequencies obtained from Ref. 40.
[d]Reference 41.
[e]See the text for details.
[f]Taken from TS1 in Ref. 31.
[g]Reference 38.
[h]Reference 39.

cussed in detail previously[37] and requires molecular constants for the energized molecule (EM) and transition state (TS) leading to the product of interest. For the primary reactions leading to Fe_nD^+ and $Fe_nCD_2^+$ formation in reactions (1) and (4), the EM is the transiently formed $Fe_nCD_4^+$ complex, which we assume has a $DFe_nCD_3^+$ structure, for reasons discussed below. For production of the secondary products, Fe_nC^+ and Fe_nCD^+ in reactions (2) and (3), we presume that the rate limiting step is the second step, i.e., decomposition of the primary $Fe_nCD_2^+$ product. Although it is possible that the rate-limiting step is the formation of the $Fe_nCD_2^+$ species, this seems unlikely at the elevated energies needed to form these two products. The EM for the production of $Fe_{n-1}D^+$ depends on whether reaction (6a) or (6b) is operative. When reaction (6a) is active, the EM should be $D_3CFe_nD^+$, whereas the EM is Fe_nD^+ when the product is formed in reaction (6b). Cross sections were modeled using both assumptions. For the $Fe_{n-1}CD_2^+$ products observed for the $n=2-14$ clusters, the EM is $Fe_nCD_2^+$. As discussed above, the $Fe_{n-1}CD^+$ and $Fe_{n-1}C^+$ products have two possible precursors: (i) Fe_nCD^+ and Fe_nC^+, respectively, can lose an Fe atom, and (ii) $Fe_{n-1}CD_2^+$ can lose D and D_2, respectively. The behavior of the cross sections indicates that the latter mechanism probably dominates; hence, the cross sections are modeled using only this assumption. Analyses using the alternate mechanism did not yield appreciably different results within experimental error.

The vibrational frequencies for these various EMs are listed in Table I and estimated as follows. For all species, the $3n-6$ vibrations associated with the cluster are assumed to equal those of the bare cluster and are estimated using a Debye model.[32] For Fe_nD^+, three additional frequencies are needed and are taken from our study of the reactions of Fe_n^+ with D_2.[13] In this work, the deuterium was assumed to bind in a bridging position (although this assumption is not critical to the final frequencies obtained). The wagging (725 cm^{-1}) and asymmetric stretching (870 cm^{-1}) frequencies were estimated from the symmetric stretching frequency (950 cm^{-1}) using a simple analysis. The ratios of the symmetric stretch to the asymmetric stretch (0.92) and to the wag (0.76) are used to estimate similar frequencies in several of the systems of interest here. For Fe_nC^+, we increase the frequency of the Fe–CD stretch measured by Chang *et al.*[38] (648 cm^{-1}) by the ratio of the masses of the ligands, which yields 750 cm^{-1}. This estimate is reasonable given the observation made below that the carbide and carbyne bond energies are similar. The two additional frequencies for the wag and asymmetric stretch of Fe_nC^+ are estimated using the ratios from Fe_nD^+. For Fe_nCD^+, the CD stretch is presumed to be unperturbed from free CD (2100 cm^{-1})[39] and a cluster–ligand stretch and bend are taken from values measured for DFeCD (648 and 503 cm^{-1}).[38] The two remaining frequencies needed, the Fe_n^+–CD wag and asymmetric stretch, are estimated using the ratios from Fe_nD^+. For $Fe_nCD_2^+$, five of the frequencies (three vibrations of CD_2, the Fe–C stretch, and an out-of-plane bend) are taken from measurements of $FeCD_2$.[38] The remaining four frequencies are scaled from the Fe–C stretch and out-of-plane bend using the ratios from Fe_nD^+. For the D_3C–Fe_n^+–D intermediate, the total number of vibrational frequencies is $(3n-6)+15$. Three of the additional 15 frequencies are associated with the Fe_n^+–D motions and are taken from our previous work.[13] Six of these are associated with the internal motions of CD_3 and are taken as equal to those for free CD_3.[40] The stretching frequency for Fe_n–CD_3 was taken to equal the comparable value in $DFeCD_3$,[41] and two additional modes were decreased from the stretching frequency using Fe_nD^+ ratios. The three final frequencies were set to 540 cm^{-1}. This is taken from the Fe–CH_3 rock frequency in the $HFeCH_3$ molecule.[41] In all cases, the cluster–ligand frequencies were

assumed to remain constant for all cluster sizes. Although this is undoubtedly not precise, clusters differing by only one iron atom should have frequencies that do not differ appreciably. Further, in our analysis of the data, we scaled all the frequencies by ±25% to account for the uncertainty in the estimation of the frequencies.

The statistical treatment of lifetime effects also requires knowledge of the transition states for each reaction of interest. For most reactions, we assume a loose transition state (LTS) located at the centrifugal barrier, a so-called phase space limit (PSL) or orbiting transition state, which is treated variationally as described in detail elsewhere.[37] For ion–molecule reactions having no barriers in excess of the reaction endothermicity, this is a reasonable assumption.[34] For LTSs, the frequencies needed are simply those of the products and are listed in Table I. For all the reactions except processes (1), (2), and (10), product cross sections were analyzed by removing the energy needed to generate the precursor (EM) for the process under consideration. For instance, during the analysis of Fe_nC^+ product cross section, the threshold energy measured for the $Fe_nCD_2^+$ precursor is removed from the total energy as that energy is not available for D_2 loss from $Fe_nCD_2^+$.

$Fe_nCD_2^+$ product cross sections were analyzed using both an LTS and a tight TS (TTS).[37] The TTS may be appropriate in this case because a barrier in excess of the endothermicity has been observed in the dehydrogenation of methane by atomic Fe^+.[31,42] This barrier is associated with a four-centered transition state, and an analogous species is the assumed TTS for all clusters here. Most cluster–ligand frequencies were assumed to equal those estimated for the analogous four-centered TS in the $Fe^+ + CD_4$ dehydrogenation reaction.[31] Three additional frequencies needed are associated with Fe_n^+–D motions and are taken by scaling 950, 870, and 725 cm^{-1} frequencies by 0.5 to account for the decreased bond order in the TTS. For dissociation of the $DFe_nCD_3^+$ intermediate to $Fe_nD^+ + CD_3$, an LTS is appropriate; however, the thresholds for this Fe_nD^+ product channel are affected by the competition with the dehydrogenation reaction channel which passes through the same intermediate, as discussed below. For some clusters, the competition is evident from the energy dependence of the cross sections, as noted above, whereas for others, the effects of competition are less clear. We consider this possibility by analyzing the data in all cases using a statistical model for competition detailed elsewhere.[43]

Fe_nC^+ product cross sections from reaction (2) were also analyzed using both LTS and TTS models, because the mechanism for the first dehydrogenation of $Fe_nCD_4^+$ to form $Fe_nCD_2^+$ should be similar to the second dehydrogenation of $Fe_nCD_2^+$ to form Fe_nC^+. Most cluster–ligand frequencies were taken from the analogous four-centered TS for dehydrogenation of D–Fe_n^+–CD_3 to form $Fe_nCD_2^+$, Table I. For reactions in which an Fe atom is lost to form $Fe_{n-1}CD_x^+$ products, there are two reasonable choices for the type of transition state: either an LTS or a somewhat tighter transition state, which has been dubbed a "standard" TS (STS),[44] similar to that assumed for dissociation of bare iron clusters.[25] The former type of transition state was assumed in our previous work on the reactions of iron cluster cations with O_2 and CO_2,[13,15] which yielded reasonable cluster oxide bond energies. Both assumptions are explored in this work.

Rotational constants for the various EMs and transition states were assumed to equal those of the bare clusters for all species except those involving the iron dimer and trimer. Rotational constants for $Fe_2CD_x^+$ and $Fe_3CD_x^+$ were estimated explicitly, as illustrated here for the examples of $Fe_2CD_3^+$ and $DFe_2CD_3^+$. We assume that both of these have C_{3v} symmetry with bond lengths of 2.0 Å for Fe–Fe,[45] 2.1 Å for Fe–C, 1.1 Å for C–D, and 1.6 Å for Fe–D.[46] These yield rotational constants of A ~2.6 cm^{-1} and B=C~0.1 cm^{-1} for both species. For the trimer species, the metal framework is assumed to have an equilateral triangular structure with Fe–Fe bond lengths of 2.0 Å.

Optimized fitting parameters of Eq. (13) for the analyses of all reaction cross sections ($n=2-15$) are given in Ref. 29 as Tables S1–S14, respectively.

B. Primary and secondary reactions

A fortunate aspect of cluster studies is the observation of identical product ions formed in both primary and secondary reactions. Thus, a species like Fe_nL^+ is formed as a primary product of Fe_n^+ in reaction (14), and a secondary product of Fe_{n+1}^+ in reactions (15) or (16)

$$Fe_n^+ + CD_4 \rightarrow Fe_nL^+ + CD_4\text{–L}, \tag{14}$$

$$Fe_{n+1}^+ + CD_4 \rightarrow Fe_nL^+ + Fe + CD_4\text{–L}, \tag{15}$$

$$Fe_{n+1}^+ + CD_4 \rightarrow Fe_nL^+ + Fe(CD_4\text{–L}). \tag{16}$$

Hence, we have at least two independent means of determining the thermochemistry of each of the Fe_nL^+ products. It is conceivable that thresholds obtained for the secondary reactions (15) could be higher than thermodynamic values, if the total energy available in reaction (15) is not efficiently retained by $Fe_{n+1}L^+$, the primary product acting as the EM in the secondary reaction. However, if we assume the energy is divided among the primary products statistically, we can expect that the $Fe_{n+1}L^+$ product will retain much more energy than the CD_4–L product, which has many fewer degrees of freedom. Similar considerations hold for alternate mechanistic pathways for the secondary reactions. Clearly, this assumption could degrade for the smallest clusters and we explicitly consider this question below.

Bond energies of interest can be obtained from the thresholds for reactions (14)–(16) using Eqs. (17)–(19)

$$D(Fe_n^+\text{–L}) = D(CD_4\text{–L}) - E_0(14), \tag{17}$$

$$D(Fe_n^+\text{–L}) = D(CD_4\text{–L}) + D(Fe_n^+\text{–Fe}) - E_0(15), \tag{18}$$

$$D(Fe_n^+\text{–}L) = D(CD_4\text{–L}) + D(Fe_n^+\text{–Fe}) - E_0(16) - D[\text{Fe–}(CD_4\text{–L})], \tag{19}$$

where $D(CD_4\text{–L})$ is the energy required to remove L from CD_4. In Eqs. (18) and (19), the dissociation energies for the bare Fe_n^+ clusters are taken from previous studies in our laboratory.[25] In the present work, neutral Fe–(CD_4–L) spe-

TABLE II. Fe_n^+–D bond energies (eV) obtained from the literature and analyses of reactions (1) and (6).

	Fe_n^+–D[a]	Fe_n^+–D (1)[b]	Fe_n^+–D (6a)[c]	Fe_n^+–D (6b)[c]
1	2.16±0.06[d]			2.22±0.14
2	1.45±0.09	1.32±0.15		1.53±0.20
3	1.77±0.15	2.02±0.09		2.13±0.22
4	2.16±0.14	2.25±0.09		2.14±0.27
5	1.90±0.17	2.21±0.09		2.05±0.32
6	2.74±0.21	2.35±0.08		2.70±0.35
7	2.11±0.19	2.18±0.10		2.26±0.34
8	1.97±0.18	2.04±0.10	2.06±0.45	3.45±0.45
9	2.38±0.17	2.30±0.08	2.25±0.48	2.42±0.44[e]
				4.14±0.44
10	2.68±0.17	2.47±0.09	2.49±0.50	2.70±0.50[e]
				4.53±0.50
11	2.52±0.15	2.42±0.08	2.77±0.58	4.15±0.50
12	2.54±0.14	2.31±0.10	3.04±0.78	4.42±0.68
13	2.52±0.12	2.52±0.10		
14	2.52±0.12	2.45±0.10		
15	2.87±0.15	2.54±0.10		

[a]Reference 13.
[b]Values obtained from analyses of reaction (1) assuming LTS and explicit competition with reactions (4).
[c]Average bond energies obtained from analyses of $Fe_{n-1}D^+$ cross sections assigned to reactions (6a) or (6b) assuming LTS and STS models.
[d]Reference 31.
[e]Bond energies obtained from analyses of $Fe_{n-1}D^+$ cross sections assigned to reaction (6b) after subtracting cross-section features corresponding to reaction (6a).

cies observed include only FeD and $FeCD_3$, which have bond energies of 1.52±0.04 eV[47] and 1.40±0.30 eV,[48] respectively.

C. Thermochemical results

1. Fe_n^+–D

Bond energies for Fe_nD^+ have previously been measured by threshold analyses of the endothermic reactions of Fe_n^+ clusters with D_2.[13] In the present study, this thermochemistry can be obtained from analyses of the cross sections for reactions (1), (6a), and (6b). Needed thermodynamic information includes $D(CD_3–D)=4.58±0.01$ eV[49] and $D(Fe–CD_3)=1.40±0.30$ eV.[48] For reaction (1), we analyzed the Fe_nD^+ cross sections using three different assumptions. First, an LTS was assumed, which is consistent with the observation that no barrier for this process is observed in the reaction of Fe^+ with methane.[30] The LTS assumption leads to bond energies about 1 eV smaller than previously reported values[13] for clusters larger than the trimer. Second, we assumed a TTS, which led to bond energies in reasonable agreement with our previous values, mean absolute deviation (MAD)=0.18±0.16 eV for $n=2–15$; however, a TTS is difficult to justify mechanistically as loss of a methyl is likely to involve a simple bond cleavage. Finally, we assumed an LTS coupled with explicit consideration of the competition[43] with the low energy dehydrogenation channel, reaction (4), assumed to have a TTS. Bond energies obtained from this last procedure are listed in Table II and shown as open circles in Fig. 15s of Ref. 29. These values are in slightly better agreement with the previous data[13] (MAD =0.16±0.12 eV for $n=2–15$) than the TTS values. Thus, this last approach is mechanistically reasonable and gives good thermodynamic results, but at the cost of a more complicated analysis. It is worth stressing that the competition threshold analysis has no additional optimizing parameters (other than the threshold energies for each channel) to adjust compared to the normal threshold analysis (including lifetime effects).[43] The competition between channels is determined by the ratio of the unimolecular rate constants for each process, as calculated using RRKM theory. Thresholds for both reactions (1) and (4) are simultaneously obtained in this procedure.

Fe_n^+–D bond energies obtained from analyses of the secondary reaction (6b) are listed in Table II (see also Fig. 15s of Ref. 29). As discussed above, the data for reaction (6b) were analyzed assuming both an LTS and an STS. The average bond energies obtained using these two models are in good agreement with the previously published values[13] up to $n=7$ (MAD=0.12±0.12 eV for $n=1–7$). Hence, our assumption that energy is efficiently retained by the primary product (Fe_nD^+) appears to be reasonable, even for these smaller clusters. For clusters larger than $n=7$, modeling of the $Fe_{n-1}D^+$ cross sections over extended energy regions using Eq. (13) requires large values of the parameter N and leads to thresholds corresponding to bond energies that are too large; see Table II (see also Fig. 15s of Ref. 29). For the values $n=8–12$, these bond energies exceed the literature values by an average of 1.70±0.21 eV, comparable to the Fe–CD_3 bond energy of 1.40±0.30 eV.[48] Hence, contributions to these cross sections from reaction (6a) are clearly indicated. Therefore, we analyze the cross sections at the lowest energies and assign these thresholds to reaction (6a), Tables S1–S12 (Ref. 29). This leads to the bond energies given in Table II and shown in Fig. 15s of Ref. 29. For reaction of Fe_{10}^+ and Fe_{11}^+, it was possible to model the contributions from both reactions (6a) and (6b) separately, such that thresholds for each could be obtained. In these two cases, bond energies for Fe_9D^+ and $Fe_{10}D^+$, respectively, derived from the thresholds for reaction (6b) (listed in Table II) also agreed nicely with the literature bond energies.

2. Fe_n^+–CD_3

Iron cluster methyl cations are observed only in the reactions of the dimer and trimer cations as secondary products, i.e., yielding $FeCD_3^+$ and $Fe_2CD_3^+$, respectively. The thresholds for these processes (Tables S1 and S2, Ref. 29) are 3.43±0.14 and 2.84±0.10 eV, respectively. If we assume that the cluster methyl cation products are formed along with FeD in reaction (10), Eq. (19) can be used to convert these thresholds to bond energies of 2.37±0.18 eV for Fe^+–CD_3 and 1.89±0.16 eV for Fe_2^+–CD_3. The value for $FeCD_3^+$ agrees well with a bond energy previously determined for $FeCH_3^+$, 2.37±0.05 eV.[11] Clearly, $FeCD_3^+$ is formed in process (10) along with FeD as a neutral product for reaction of the dimer. This pathway also seems certain for the trimer reaction because the resulting Fe_2^+–CD_3 bond energy is similar to the Fe_2^+–D bond energy, Table II. The alternate assumption of concomitant formation of Fe+D yields a bond energy of 3.9±0.2 eV for Fe_2^+–CD_3, much too large to be reasonable. Larger clusters do not produce $Fe_{n-1}CD_3^+$ with

any efficiency, apparently because they have more facile decomposition pathways than loss of FeD from the transient $Fe_nCD_4^+$ intermediate.

3. $Fe_n^+ - CD_4$

For clusters with $n \geq 10$, we observe an $Fe_nCD_4^+$ product. Unfortunately, because of their small magnitudes, the quality of these cross sections is not sufficient to analyze using Eq. (13). However, as discussed in detail in our work on the reactions of Fe_n^+ with D_2, where analogous $Fe_nD_2^+$ adducts were observed,[13] the apparent threshold of such products is a reasonable measure of the true threshold because the internal energy of the reactant clusters is not active in producing these species. Qualitatively, the thresholds for the $Fe_nCD_4^+$ products for $n \geq 10$ lie in the vicinity of 0.9 ± 0.3 eV. The structure of a $Fe_nCD_4^+$ species could correspond to a physisorbed methane molecule, $Fe_n^+(CD_4)$, or to a chemisorbed species, $D-Fe_n^+-CD_3$ or some other variant. A physisorbed species should exhibit no activation barrier to its formation because the cluster ion and methane have an attractive ion-induced dipole interaction. Therefore, it seems likely that the cross section observed corresponds to a chemisorbed structure, which means that the threshold corresponds to the activation energy for chemisorption, probably a C–D bond activation in the present cases. Assignment of these species to chemisorbed methane would help explain why such species are observed, as their lifetime must exceed the $\sim 10^{-4}$ s flight time of the ions in our instrument. A physisorbed species should have a fairly short lifetime because loss of an intact methane molecule should be facile. However, if desorption of methane to return to reactants requires coupling of two or more fragments, which may now be remote from each other on the cluster surface, then the lifetime of $Fe_nCD_4^+$ species could increase dramatically. This is especially true for the largest clusters, where the energy needed to eliminate methane has been dissipated throughout the cluster. Finally, Anderson[10] calculated an activation energy of about 0.9 eV for the chemisorption of methane on Fe_2, which is consistent with our observations of the magnitude for such an activation energy.

4. $Fe_n^+ - CD$ and $Fe_n^+ - C$

Bond energies for $Fe_n^+ - CD$ can be obtained from analyses of reactions (3) and (8). The required thermochemistry is $D(CD_4\text{–}L) = D(CD_2\text{–}D_2) + D(CD\text{–}D) = 9.25 \pm 0.04$ eV.[49] For reaction (3), the precursors are the primary $Fe_nCD_2^+$ products, while for reaction (8) they are the $Fe_{n-1}CD_2^+$ products, as discussed above. Therefore, cross sections are analyzed for thresholds using an LTS model associated with D atom loss for both reactions (3) and (8) and the results are given in Table III and also shown in Fig. 16s of the supplementary materials.[29] Bond energies obtained from analyses of reaction (8) are systematically lower compared to the bond energies obtained from reaction (3), with a MAD of about 0.47 ± 0.15 eV for $n = 1-11$. Because these differences are within the combined experimental errors (which average 0.56 eV), this is some indication that there are no significant reverse barriers for either process. Of these various bond energies, those obtained from analyses of reactions (3) are the most reliable for several reasons. (a) The mass overlap adjustments for the Fe_nCD^+ cross sections are less ambiguous compared to cross sections for $Fe_{n-1}CD^+$ formed in reaction (8). (b) Thresholds for reaction (8) occur at high energies, such that there are fewer data points for modeling given our energy range of about 10 eV (CM). (c) Thresholds for reaction (8) could be shifted to higher energies by competition with the more efficient low-energy processes or shifted as a consequence of the multiple neutral products carrying away excess energy.

TABLE III. $Fe_n^+ - CD$ bond energies (eV) obtained from analyses of reactions (3) and (8).

n	$Fe_n^+ - CD$ (3,LTS)	$Fe_n^+ - CD$ (8,LTS[a])
1	4.38 ± 0.30[a]	3.93 ± 0.32
2	3.04 ± 0.13	3.32 ± 0.20
3	5.11 ± 0.10	4.61 ± 0.36
4	5.10 ± 0.30	4.72 ± 0.28
5	5.26 ± 0.22	5.03 ± 0.45
6	5.34 ± 0.17	4.86 ± 0.49
7	4.88 ± 0.24	4.25 ± 0.58
8	5.08 ± 0.25	4.46 ± 0.56
9	5.03 ± 0.35	4.55 ± 0.67
10	4.95 ± 0.40	4.56 ± 0.67
11	5.70 ± 0.31	4.95 ± 0.86
12	5.60 ± 0.37	
13	5.95 ± 0.35	
14	6.35 ± 0.39	
15	5.75 ± 0.40	

[a]R. L. Hettich and B. S. Freiser, J. Am. Chem. Soc. **106**, 2537 (1986).

Bond energies for $Fe_n^+ - C$ can be obtained from analyses of reactions (2) and (7). Here, the required thermochemistry is $D(CD_4\text{–}L) = D(CD_2\text{–}D_2) + D(C\text{–}D_2) = 8.20 \pm 0.04$ eV.[49] Thresholds for reactions (2) and (7) are analyzed using $Fe_nCD_2^+$ and $Fe_{n-1}CD_2^+$, respectively, as the precursors with both LTS and TTS models. Bond energies obtained from reaction (7) using the LTS model do not agree well within experimental uncertainties with results obtained from analyses of reaction (2) using either the LTS or TTS models. Hence, we conclude that reaction (7) proceeds via a TTS, an assumption that leads to consistent thermochemistry with that derived from reactions (2). Because reactions (2) and (7) both involve dehydrogenations from $Fe_nCD_2^+$ intermediate products, they should have analogous mechanisms. Bond energies obtained using a TTS model for reactions (2) and (7), Table IV, Fig. 17s of Ref. 29, agree well with one another (MAD $= 0.32 \pm 0.21$ eV), well within experimental uncertainties. The BDEs derived from the secondary processes (7) are generally lower than those obtained from reactions (2), comparable to the trends observed for the $Fe_n^+ - CD$ bond energies, as noted above. Thresholds from the primary reactions (2) are more precise and therefore taken to be our best determination of bond energies. Reasons for the higher reliability are the same as those listed above for the $Fe_n^+ - CD$ bond energies.

One interesting observation is that the BDE obtained from reaction (7) for $Fe_{12}C^+$ is much greater than that from reaction (2), in contrast to all the other clusters, $n = 2-13$,

TABLE IV. Fe_n^+–C bond energies (eV) obtained from analyses of reactions (2) and (7).

n	Fe_n^+–C (2,TTS)	Fe_n^+–C (7,TTS)
1	4.08±0.30[a]	
2	4.13±0.30	3.97±0.36
3	5.31±0.14	4.66±0.14
4	5.84±0.04	5.68±0.04
5	5.88±0.05	5.56±0.34
6	5.79±0.10	5.69±0.43
7	5.40±0.15	5.16±0.38
8	5.63±0.15	5.47±0.49
9	5.86±0.16	5.38±0.61
10	5.99±0.18	5.43±0.53
11	6.05±0.20	6.02±0.62
12	5.92±0.18	6.47±0.69
13	6.15±0.22	5.71±0.69
14	6.24±0.21	
15	6.00±0.26	

[a]R. L. Hettich and B. S. Freiser, J. Am. Chem. Soc. **106**, 2537 (1986).

TABLE V. Fe_n^+–CD_2 bond energies (eV) obtained from analyses of reactions (4) and (9).

n	Fe_n^+–CD_2 (4,LTS)	Fe_n^+–CD_2 (4,TTS)	Fe_n^+–CD_2 (9)[a]
1		3.11±0.10[b]	3.60±0.15
2	2.17±0.17	2.29±0.15	3.39±0.18
3	2.66±0.09	2.97±0.09	2.97±0.22
4	3.29±0.09	3.50±0.09	3.69±0.25
5	3.00±0.09	3.40±0.09	3.72±0.27
6	~2.7	~3.2	3.82±0.29
7	2.45±0.09	3.07±0.09	3.54±0.29
8	2.86±0.09	3.24±0.09	3.71±0.34
9	3.08±0.09	3.49±0.09	3.92±0.34
10	3.25±0.09	3.61±0.09	4.17±0.36
11	3.20±0.09	3.64±0.09	4.49±0.41
12	3.16±0.09	3.59±0.09	5.01±0.48
13	3.14±0.09	3.56±0.09	4.18±0.48
14	3.16±0.09	3.58±0.09	···
15	3.11±0.09	3.57±0.09	···

[a]Average bond energy obtained from LTS and STS models.
[b]Reference 31.

where the values from reaction (7) are lower than those from reaction (2), Table IV, Fig. 17s of Ref. 29. Direct comparison of the cross sections for reaction (7) with the $n=9-13$ reactant clusters indicates that the apparent threshold for $n=13$ is considerably higher than those for the other clusters, properly reflecting the enhanced stability of Fe_{13}^+ compared with the other clusters of comparable size (by 1.3±0.2 eV compared to $n=9$, 10, and 14).[25] However, the analysis of this cross section reduces the difference between thresholds considerably such that the bond energy derived using Eq. (18) appears unduly influenced by the contribution of the $D(Fe_n^+-Fe)$ term in this equation. Of course, it is possible that the Fe_{12}^+–C bond is particularly strong for the same reason that the Fe_{12}^+–Fe bond is strong, although we have speculated that this is because of the high symmetry of the Fe_{13}^+ cluster,[13,25] which could not be true of $Fe_{12}C^+$. However, the enhanced strength of the Fe_{12}^+–C bond is not confirmed by the thermochemistry obtained using reaction (2). Hence, we believe that the Fe_{12}^+–C BDE obtained from the secondary reaction (7) is particularly high because of difficulties in the analysis of this process. To a lesser extent, this appears to be true for the Fe_{11}^+–C bond energy as well.

5. Fe_n^+–CD_2

Bond energies for Fe_n^+–CD_2 can be obtained from analyses of the thresholds for reactions (4) and (9) using Eqs. (17) and (18), respectively, and $D(CD_2-D_2)=4.82$ ±0.03 eV.[49] As discussed above, the data for reaction (4) were analyzed assuming both an LTS and a TTS. Competition with reaction (1) is also explicitly considered but this does not alter the thresholds obtained for reaction (4). The resultant bond energies are listed in Table V. We find that the values derived assuming an LTS are an average of 0.44 ±0.07 eV lower than those for a TTS for $n=5-15$. One means of determining which of these sets of values is more accurate is to examine the results obtained from analyses of the secondary reactions (9). In these cases, the reactions correspond to loss of an Fe atom from the $Fe_nCD_2^+$ primary product, such that the transition states may be treated with loose or standard transition state models, as outlined above.

For reaction of Fe_2^+ to form $FeCD_2^+$ in process (9), the threshold obtained using an LTS model corresponds to an Fe^+–CD_2 bond energy of 3.56±0.15 eV, in good agreement with the literature bond energy, 3.57±0.04 eV.[31,50] However, this result is not sensitive to the nature of the transition state assumed as the STS model yields a bond energy of 3.64 ±0.15 eV, also in agreement. These bond energies lie above that derived from the threshold measurement of reaction (4) with $n=1$. As noted above, we have demonstrated that there is a barrier of 0.42±0.11 eV to reaction (4) for the monomer cation by examining the reverse process, reaction of $FeCH_2^+ + H_2$.[31] This barrier is attributed to a four-center transition state,[31] as verified by theoretical calculations.[46]

For reaction of Fe_3^+ to form $Fe_2CD_2^+$, the threshold obtained from analysis of reaction (9) using an LTS corresponds to a bond energy of 3.38±0.17 eV, well above the value derived from reaction (4), Table V. Again, the result for reaction (9) is not particularly sensitive to the type of transition state as the bond energy obtained using an STS is 3.40±0.17 eV. The discrepancy between the results for the primary and secondary reactions is sensibly attributed to a barrier along the reaction path for dehydrogenation in reaction (4). This indicates that the use of the TTS model for reaction (4) is appropriate. For reaction of the dimer cation, this barrier is measured here to be about 1.10±0.23 eV, using the threshold for reaction (4) obtained assuming a TTS. Figure 1 shows that the $Fe_2CD_2^+$ cross section is much smaller than that for Fe_2D^+ but has a comparable threshold, behavior that is consistent with a tight transition state.

For reactions of Fe_4^+ and Fe_5^+, the average $Fe_nCD_2^+$ bond energies obtained for $n=3$ and 4 from analyses of reaction (9) using LTS and STS models agree within experimental error with those obtained for reactions (4) of Fe_3^+ and Fe_4^+ using the TTS assumption in the analysis, but are inconsistent with the LTS values. This agreement indicates that the barrier no longer exceeds the endothermicity for reaction (4) by a significant amount. This is consistent with the observa-

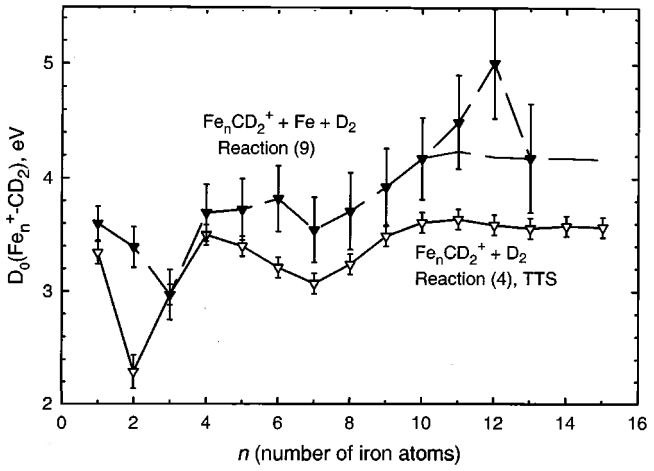

FIG. 7. $Fe_n^+-CD_2$ bond energies (Table V) obtained from analysis of reactions (4) (open triangles) and (9) (solid triangles).

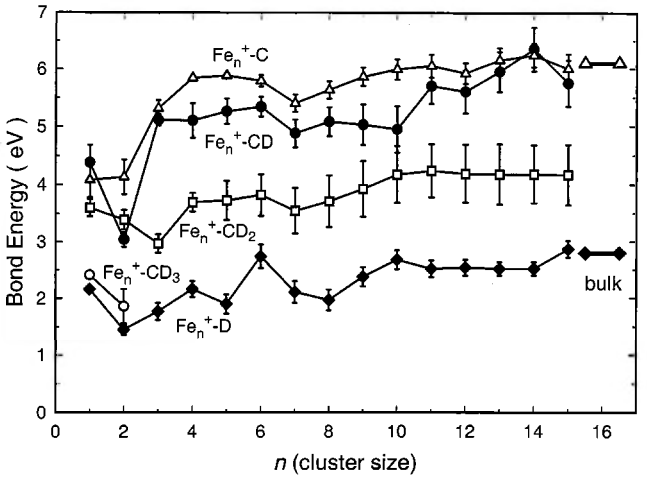

FIG. 8. Comparison of bond energies for Fe_n^+-D (solid diamonds, taken from Ref. 13), $Fe_n^+-CD_3$ (open circles, Ref. 11 and this work), $Fe_n^+-CD_2$ (open squares, this work, Table V, see the text), Fe_n^+-CD (solid circles, this work, Table III), and Fe_n^+-C (open triangles, this work, Table IV). Bulk phase values for iron surfaces binding D (Refs. 62 and 63) and an estimate for C (Ref. 63) are also shown.

tion that the cross sections for $Fe_3CD_2^+$ and $Fe_4CD_2^+$, Figs. 2 and 3, have appreciable magnitudes and thresholds that are lower than those for the Fe_nD^+ product. As previous experiments[51–53] have demonstrated that the iron tetramer cation is much more reactive than other iron clusters, it seems reasonable that there should not be a barrier in excess of the endothermicity for the dehydrogenation reaction by the tetramer.

For larger clusters, $n>5$, the bond energies obtained from reaction (9) using the LTS model are slightly smaller, by an average of 0.3 ± 0.1 eV, than those obtained using the STS model. The averages of the LTS and STS results are given in Table V and are about 0.7 ± 0.3 eV larger than the bond energies obtained from reaction (4) assuming a TTS, Table V. These two sets of values are shown in Fig. 7. The relative magnitudes of these values are in direct contrast to those for Fe_nCD^+ and Fe_nC^+ bond energies, where all but one value obtained from the secondary reactions (7) and (8) were lower than those from the primary processes (2) and (3), e.g., as shown in Fig. 8. Hence, the differences between the values in Fig. 7 must be attributed to barriers for dehydrogenation, as we concluded for the monomer and dimer reactions. Given the conclusion that there is a barrier, analyses of reaction (4) using TTSs are definitely more appropriate than use of LTSs. For $n\geqslant10$ clusters, we also note that the apparent thresholds for the $Fe_nCD_2^+$ products are identical to those for $Fe_nCD_4^+$ products in all cases, e.g., Fig. 6. Given our assignment of this latter threshold to the barrier for C–D bond activation, this is another indication that the thresholds for $Fe_nCD_2^+$ formation do not correspond to the thermodynamic limits and hence that bond energies derived from the thresholds for reaction (4) are too low. As discussed below, this conclusion is also consistent with qualitative arguments concerning the relative magnitudes of the $Fe_n^+-CD_2$ bond energies compared to other $Fe_n^+-CD_x$ bond energies. Note that the assignment of the barriers for $n\geqslant10$ to the C–D activation step means that the barrier lies in the entrance channel for reaction. This is in contrast to the assignment for reactions of $n=1$ and 2, where the barrier is determined to be in the exit channel. This change in the rate-limiting step as a function of cluster size seems consistent with no or small barriers observed for reactions of $n=3$ and 4 clusters. Given the conclusion that the barrier is in the entrance channel for $n\geqslant5$, modeling of the reaction (4) cross sections assuming a four-center TTS may be inappropriate. However, modeling the $Fe_nCD_2^+$ cross sections using a TTS appropriate for C–D activation in the entrance channel did not change the TTS thresholds appreciably (by less than 0.1 eV). Hence, we conclude that our best thermodynamic values for $Fe_n^+-CD_2$ bonds come from analyses of reaction (9) and that there is a barrier of about 0.7 ± 0.3 eV in the excess of the endothermicity for the dehydrogenation reactions (4) with Fe_n^+, $n\geqslant5$.

Examination of the bond energies in Fig. 7 shows that the values obtained from analyses of reactions (4) and (9) approximately parallel one another from $n=6-13$, with the notable exception of $n=12$ and, to a lesser extent, 11. We believe the large bond energies obtained for $Fe_{12}^+-CD_2$ and $Fe_{11}^+-CD_2$ from analyses of reaction (9) may overestimate the true bond energies. The reasons parallel the discussion above for the $Fe_{12}C^+$ bond energy obtained from analysis of reaction (7) vs that from reaction (2). Although not definitive, our best estimates for $Fe_n^+-CD_2$ ($n=11$, 12, 14, and 15) bond energies are obtained by assuming a constant activation barrier of 0.6 eV for these larger clusters such that the estimated correct BDEs parallel those obtained from analyses of reaction (4), i.e., they fall around 4.2 ± 0.5 eV, Fig. 7. It is possible that the $Fe_{11}^+-CD_2$ and $Fe_{12}^+-CD_2$ bond energies are really higher than this.

V. DISCUSSION

A. Bond energies

Our recommended set of bond energies between iron cluster cations and the D and CD_x ($x=0-3$) ligands is shown in Fig. 8. The Fe_n^+-D values are taken from our previous work on reactions of $Fe_n^+ + D_2$.[13] Results from the

present study substantiate these values but analyses of the D_2 reaction cross sections are less problematic than for the CD_4 reaction system because there is no competition with other products in the D_2 system. The Fe_n^+–CD values are those derived from analyses of reaction (3) with an LTS in all cases, Table III, whereas those for Fe_n^+–C are TTS results for reaction (2), Table IV. As noted above, the latter two sets of values are substantiated reasonably well by results for the secondary reactions (8) and (7), respectively. The Fe_n^+–CD_2 values listed in Table V are obtained from reaction (9) using the average thresholds obtained from LTS and STS assumptions, except for the $FeCD_2^+$ value, which is taken from the literature,[50] and the values for $n=11$, 12, 14, and 15 which are estimated as discussed above.

In general, the trends in these cluster–ligand bond energies can be understood by considering the maximum number of bonds that the ligands can make with the cluster. $D(^2S)$ and CD_3 ($^2A_1$) can make only a single covalent bond with the cluster, while CD_2 ($^3B_2$) can make two covalent bonds. CD can make three covalent bonds, but this requires promotion to the $\tilde{a}\,^4\Sigma^-$ state, which is 0.72 eV above the $X\,^2\Pi_r$ ground state.[39] The carbon atom has a ground-state electronic configuration of $(2s)^2(2p)^2$ such that it can form two covalent bonds and accept electron density into the empty $2p$ orbital to form a third dative bond. It can be seen that the Fe_n^+–D bond energies and the Fe_n^+–CD_3 ($n=1$ and 2) bond energies are comparable, as expected. The methyl is slightly more strongly bound, which can be justified because CD_3 is more polarizable than D.[54,55] The Fe_n^+–CD_2 bond energies lie an average of 1.56±0.25 eV higher in energy than the Fe_n^+–D values for all n. Fe_n^+–CD and Fe_n^+–C bond energies, which are similar to one another, are higher than the Fe_n^+–D values by 3.03±0.41 and 3.49±0.26 eV, respectively, for $n \geqslant 3$. These observations are qualitatively consistent with formation of single (D and CD_3) versus double (CD_2) versus triple (CD and C) bonds, as anticipated from the bonding character of the ligands.

We anticipate that the cluster-carbon double bonds should be about 1.7 times stronger than the single bonds, as this is the ratio of H_3C–CH_3 to H_2C=CH_2 and M^+–CH_3 to M^+=CH_2 bond energies.[11] Cluster-carbon triple bonds should be about 2.5 times stronger, on the basis of H_3C–CH_3 to HC≡CH and M^+–CH_3 to M^+≡CH ratios.[11] In agreement with this qualitative expectation, the Fe_n^+–CD_2, Fe_n^+–CD, and Fe_n^+–C bond energies are an average of 1.7 ±0.2, 2.3±0.3, and 2.5±0.3 times stronger, respectively, than the Fe_n^+–D bond energies for $n \geqslant 3$. Note that Fe_n^+–CD_2 bond energies obtained from thresholds for reaction (4) using a TTS model are only 1.4±0.2 times larger than the Fe_n^+–D bond energies, and those derived assuming an LTS for reaction (4) are even lower, a ratio of 1.3±0.2. These results are further evidence that the thresholds measured for reaction (4) do not correspond to the thermodynamic values.

The patterns in the bond energies as a function of cluster size can be used to qualitatively probe the cluster geometry and electronic configuration, as discussed in the following sections.

1. Fe_n^+–D

In our previous work,[13] we discussed the variations in the Fe_n^+–D bonds using promotion energy arguments and this discussion will not be repeated here. In all cases, the metal–metal bonds are stronger than the metal–deuteride bonds, and for most cluster sizes the difference is about 0.3 eV, such that these bond energies largely parallel one another. This is an indication of similar bonding between Fe–Fe and Fe–D. However, Fe_5^+–Fe, Fe_8^+–Fe, Fe_{12}^+–Fe, and Fe_{14}^+–Fe, bond energies are much stronger (by >0.7 eV) than the respective Fe_n^+–D bond energies. This is believed to be because the Fe_6^+, Fe_9^+, Fe_{13}^+, and Fe_{15}^+, clusters have particularly stable geometries, such that substitution of an iron atom by D destroys the symmetry of the cluster, thereby affecting its stability.

2. Fe_n^+–CD_3

$D(Fe^+$–$CD_3)$ is larger than $D(Fe_2^+$–$CD_3)$, a result that can be explained using promotion energy arguments, as previously discussed for D atom bonding.[13] $Fe^+(^6D,4s^13d^6)$ has a favorable electronic configuration to form a strong single bond, as there is an electron in the $4s$ orbital, although single bond formation does involve the loss of exchange interactions between the $4s$ and $3d$ orbitals.[56–59] Fe_2^+ is believed to have a $\sigma_g(4s)^2(3d^{13})$ electronic configuration, formed by the combination of $Fe(4s^23d^6)$ and $Fe^+(3d^7)$.[13] Formation of a covalent bond between CD_3 (or D) and a $4s$-like orbital on the iron dimer cation is believed to require promotion of an electron from the valence $3d$ orbitals into the $\sigma_u^*(4s)$ orbital, a weakly antibonding molecular orbital. This leads to a sizable promotion energy,[13] which results in Fe_2^+–CD_3 and Fe_2^+–D bond energies that are the weakest of all clusters.

3. Fe_n^+–CD_2

Discussion of the bonding of CD_2 to iron clusters is speculative as nothing is known about the structures of these cluster species. As noted above, the bond energies of CD_2 to Fe_n^+ clusters indicate that two bonds are formed. Presumably, CD_2 could bind terminally to the cluster by forming a σ and a π bond with a single metal atom or could bridge across two metal centers by forming two σ bonds. $Fe^+(4s^13d^6)$ must bind terminally and has a bond energy weakened by the need to spin decouple the $4s$ and one $3d$ electron from the other nonbonding $3d$ electrons. This promotion energy lowers the Fe^+–CH_2 bond energy from an intrinsic metal–carbon double-bond energy of about 4.3±0.1 eV (and an intrinsic π bond energy of about 1.8 eV).[11,60] The $Fe_2CD_2^+$ bond energy exceeds the Fe_2D^+ bond energy by 1.9±0.2 eV, equal to the intrinsic metal–carbon π bond. Thus, no additional promotion is needed to form the π bond once promotion needed to form the σ bond has occurred. In contrast, Fe_3^+ has the weakest bond to CD_2 and requires additional promotion to form the π bond. Previous work has suggested a $1a_1^22a_1^2$ ($4s$-like orbital) ground electronic configuration for the trimer, which requires promotion to a $1a_1^22a_1^11b_2^1$ ($4s$-like orbital) configuration to form a single bond.[13] The $1a_1^22a_1^11b_2^1$ configuration is naturally set up to bind to an edge bridging CD_2 but requires spin decoupling both the $2a_1$ and $1b_2$ orbitals from

the $3d$ orbitals. We also find that Fe_6^+ has a particularly weak π bond to CD_2. This seems consistent with our hypothesis[13] of a $a_{1g}^2 t_{1u}^5$ ($4s$-like orbital) ground electronic configuration. This can form a reasonably strong single bond to the singly occupied t_{1u} orbital, but formation of a π bond would require decoupling of a $3d$ orbital and possibly promotion to a $4s$-like antibonding orbital of e_g symmetry. Almost all other clusters, $n=2$, 5, ≥ 8, have π bonds that are close to the intrinsic value, about 1.8 eV. Thus, formation of these bonds does not appear to require excessive electronic rearrangement.

4. Fe_n^+-CD and Fe_n^+-C

The most striking observation in the patterns of the binding of CD and C to iron cluster cations is that the values for $n \geq 3$ are large and do not vary appreciably. Bonds to the monomer and dimer cations are weaker, particularly Fe_2^+-CD. These ligands can potentially bind to clusters in three different ways: terminal, twofold bridging, and threefold bridging. An obvious implication of the strength of the bonds to the trimer and larger clusters is that binding to three atoms in a threefold site provides the strongest bond energies, consistent with the known structure of alkylidynes bound to many surfaces.[61] However, O atoms also bind strongly to Fe_n^+, $n \geq 3$,[13] indicating that this pattern is not definitive for threefold bridging. The relative bond energies of $Fe_2^+-CD_2$, Fe_2^+-CD, and Fe_2^+-C indicate that the iron dimer cation can form two covalent bonds and donate an electron pair to form a third dative bond, but that the promotion energy to form a third covalent bond is prohibitive. Theoretical studies of these molecules would be of interest in further understanding these trends.

5. Bond energies compared to bulk phase values

One area where cluster studies may provide insight into condensed phase chemistry lies in the determination of thermochemistry for species bound to surfaces. We have previously noted that bond energies of oxygen to iron clusters larger than two atoms are relatively constant at about 5.8 $\pm$0.3 eV and match bulk phase heats of adsorption of oxygen to iron surfaces, 4–5.5 eV.[13,15] Likewise, Fe_n^+-D bond energies[13] reach a relatively constant value (Fig. 8) of about 2.61$\pm$0.14 eV for $n \geq 10$. This is close to the bulk phase value for hydrogen binding to bulk iron surfaces, about 2.8 eV for measurements on Fe(100), Fe(110), and Fe(111) surfaces.[62,63]

In contrast to the atomic H and O systems, there is virtually no experimental information on the thermochemistry of organic fragments (C, CH, CH_2, and CH_3) bound to metal surfaces. The binding of C to nickel surfaces has been measured, but a value for iron surfaces (7.2 eV) has been estimated from the enthalpies of formation of bulk iron–carbides.[63] Comparison to bulk phase compounds appears to be a reasonable means to estimate adsorption enthalpies for oxides and nitrides, but insufficient data are available to assess its accuracy for carbides. Nevertheless, the estimate for iron–carbides is only somewhat larger than our Fe_n^+-C bond energies, which are on average about 6.1$\pm$0.2 eV for larger clusters ($n \geq 10$). It is possible that the estimate from carbides includes contributions from tetracoordinate C, which may not be accessible to surfaces or clusters. Certainly, the bond energy patterns noted above, specifically the agreement between our Fe_n^+-C and Fe_n^+-CD bond energies, indicate that cluster–carbides form triple bonds.

In addition, a bond order conservation—Morse potential (BOC-MP) approach, developed by Shustorovich,[64–67] has been used to estimate heats of adsorption for various species. Bell reports heats of chemisorption of H, C, CH, CH_2, and CH_3 on Fe/W(110) surfaces ("a model surface for which adsorbate binding energies are intermediate between those on Fe and W, which are closely similar") calculated from the BOC-MP approach.[68] The heat of chemisorption for H to Fe/W(110) is 2.86 eV, comparable to the values noted above from surfaces and from clusters. The value for C is 8.7 eV, substantially higher than the estimates from our cluster work (6.1$\pm$0.2 eV) or the bulk iron–carbides (7.2 eV).[63] The 8.7 eV (200 kcal/mol) value is an assumed value that is essentially extrapolated as tetracoordinate carbon from experimental data for the binding of H (monocoordinate) and N (tricoordinate) to Fe(110) surfaces.[67] On this basis, we can estimate that tricoordinate C bonding is the same as N, 6.1 eV, in good agreement with our cluster results.

The molecular species (CH, CH_2, and CH_3) are estimated using the BOC-MP approach to bind to Fe/W(110) surfaces by 6.2, 4.5, and 2.7 eV, respectively.[63] These values are in reasonable agreement with our values for larger clusters, 5.9$\pm$0.4 eV, 4.2$\pm$0.4, and 2.6$\pm$0.2 (using D as an analogy to CD_3), respectively. Overall, this agreement indicates that our bond energies for atomic (H and C) and molecular (CH, CH_2, and CH_3) species bound to larger clusters are reasonable experimental estimates of the binding energies on surfaces.

B. Reaction mechanism

To understand the mechanism of the reactions of iron cluster cations with methane, we reexamine what is known about the reactions of atomic Fe^+ with CH_4,[30,42] because the basic principles involved should be the same. This reaction occurs by C–H bond activation to form a $H-Fe^+-CH_3$ intermediate, which can decompose by simple bond cleavage to form $FeH^+ + CH_3$ or $FeCH_3^+ + H$. The former channel is favored because of conservation of angular momentum effects.[30] The lowest energy process is dehydrogenation, which involves rearrangement of the $H-Fe^+-CH_3$ intermediate to a four-centered transition state involving an incipient H–H bond.[42,46] The energy of this transition state has been measured to lie 0.42$\pm$0.06 eV above the $FeCH_2^+ + H_2$ product asymptote.[31] Because the FeH^+ and $FeCH_2^+$ products share the common $H-Fe^+-CH_3$ intermediate, they compete directly with one another. The hydride channel dominates at higher energies because simple cleavage of the Fe–C bond is kinetically more facile than rearrangement over the tight four-centered transition state needed for dehydrogenation.

The electronic requirements for sigma bond activation of CD_4 at a transition metal center can be viewed fairly simply. In order to break the C–D covalent bond and simultaneously

form two new bonds between the metal and the D and CD_3 fragments, the metal center must accept electron density from the C–D bond and donate electron density into the antibonding orbital of this bond. Formally, this is an oxidative addition process in which the metal oxidation state increases by 2, although neither the D or CD_3 ligands will carry a full negative charge. For atomic first row transition metal ions, the acceptor orbital is largely the $4s$ orbital, while the donor is a $3d\pi$. Combining these orbitals with the bonding and antibonding σ orbitals of the C–D bond leads to pairs of bonding and antibonding molecular orbitals (MOs) for the $D–Fe^+–CD_3$ intermediate. To create the most favorable bonding situation, four electrons are needed to occupy the bonding MOs with no additional electrons for the antibonding MOs. As the C–D bond provides two electrons, the metal must have an empty σ-acceptor and a doubly occupied π-donor. For atomic Fe^+, this explains why the $^4F(3d^7)$ state is about 20 times more reactive than the $^6D(4s^13d^6)$ state. Further, insertion of $Fe^+(^4F)$ into the sigma bond of CD_4 to form the ground-state quartet $D–Fe^+–CD_3$ intermediate is spin-allowed.

1. $Fe_nCD_4^+$ products

In analogy with the mechanism for reaction of the monomer with methane, the first step in the reaction of the iron cluster cations with CD_4 is C–D bond activation to form a $D–Fe_n^+–CD_3$ intermediate. The observation of $Fe_nCD_4^+$ products for $n \geqslant 10$ that can be assigned to chemisorbed intermediates is clearly consistent with this hypothesis. The energy needed to activate the C–H bond in CH_4 on two Fe atoms, as calculated by Anderson,[10] is 0.91 eV, which is in good agreement with the thresholds observed for $Fe_nCD_4^+$ formation for $n \geqslant 10$. The overall thermodynamics for forming the $D–Fe_n^+–CD_3$ intermediates can be estimated by simple bond additivity as equal to $D(D–CD_3)–2D(Fe_n^+–D)$, where we assume $D(Fe_n^+–CD_3) \approx D(Fe_n^+–D)$. This estimate assumes that binding D to the cluster does not affect the binding of CD_3 to the cluster and vice versa, which seems reasonable for larger clusters because each ligand can find a binding site remote from the other ligand. Given this assumption, we estimate that formation of $DFe_nCD_3^+$ is exothermic for $n=6$ and $n \geqslant 9$, and endothermic by less than 0.9 eV for all other clusters except $n=2$ and 3. Thus, the thresholds observed for formation of $DFe_nCD_3^+$ ($n \geqslant 10$) can be attributed to barriers for $D–CD_3$ bond activation. We have observed similar activation barriers for reactions of D_2 with Cr_n^+ and Fe_n^+.[16,19]

The oxidative addition of the C–D bond to the metal cluster formally increases the effective charge on the cluster, such that smaller clusters with more charge density might be expected to exhibit larger barriers to this process. It is difficult to assess whether such a trend might be exhibited in the present results. Observations for the smallest clusters ($n=2$ and 3) are limited by exit channel barriers for the reductive elimination reaction (4). For the larger clusters studied, $n \geqslant 10$, barriers are clearly present for the oxidative addition reaction to form $Fe_nCD_4^+$ species. These barriers are comparable for $n=10–15$, exhibiting no obvious trend with cluster size.

2. Fe_nD^+ and $Fe_{n-1}CD_3^+$ products

From a $D–Fe_n^+–CD_3$ intermediate, the major ionic product at higher energies, Fe_nD^+, can be formed by cleaving the Fe–C bond and eliminating an intact methyl group. Once this product is formed, the cross sections for products formed at lower energies ($Fe_nCD_2^+$ and Fe_nCD^+) begin to decline, Figs. 1–6, indicating competition between these channels. This competition is also indicated by the fact that accurate Fe_nD^+ bond energies are obtained from the observed thresholds only when competition with dehydrogenation is explicitly considered. The observation of this competition is consistent with all reaction channels sharing the putative $D–Fe_n^+–CD_3$ species as a common intermediate.

Unlike the monomer,[30] larger iron clusters do not form a $Fe_nCD_3^+$ product. This is likely to be a matter of experimental sensitivity combined with the fact that formation of this product is inhibited by angular momentum conservation considerations. Simply, the reduced mass of the $Fe_nCD_3^+ + D$ product channel is about 2 amu, while that for the $Fe_nD^+ + CD_3$ product channel approaches 18 amu, comparable to the reduced mass of the $Fe_n^+ + CD_4$ reactants (about 20 amu). Because orbital angular momentum is largely conserved in these bimolecular reactions, the phase space available to the $Fe_nCD_3^+ + D$ product channel is much smaller than that associated with the $Fe_nD^+ + CD_3$ product channel.

As shown above by thermodynamic arguments, small amounts of $FeCD_3^+ + FeD$ and $Fe_2CD_3^+ + FeD$ are observed for reactions of the dimer and trimer, respectively. Clusters larger than Fe_8^+ show an additional path to the formation of $Fe_{n-1}D^+$ corresponding to loss of $FeCD_3$ neutral. These two observations provide direct evidence that C–D bond activation by metal clusters produces an intermediate where the D and CD_3 ligands are bound to *different* iron atoms. It seems likely that this is true for all clusters, even though comparable observations are not made for $n=4–7$. The failure to observe the $Fe_{n-1}CD_3^+$ products for larger clusters, $n>3$, and $FeCD_3$ loss for smaller clusters, $n<9$, is not understood.

3. $Fe_nCD_2^+$ products

As noted above, competition between $Fe_nCD_2^+$ and Fe_nD^+ product channels indicates that they share a common intermediate, presumably $DFe_nCD_3^+$. For $n=1$, the dehydrogenation reaction (4) is known to occur by a four-centered transition state evolving from this intermediate and lying in the exit channel. This TTS has been measured to lie 0.42 eV above the products.[31] For the dimer reaction, dehydrogenation is also found to have a barrier, which lies about 1.10 $\pm$0.23 eV above the $Fe_2CD_2^+ + D_2$ products. It is possible that this barrier again corresponds to a four-centered elimination from the intermediate in which both ligands are attached to the same iron atom. However, another possibility is that the reaction occurs by a five-centered elimination from a $DFe–FeCD_3^+$ intermediate. Complicating factors in thinking about the likely pathway is whether any of the ligands, D, CD_2, or CD_3, are bridging rather than terminal. Without other information, no definitive conclusions regarding the mechanism of the dehydrogenation process by the iron dimer cation can be made.

For the dehydrogenation reactions (4) of the trimer cation and tetramer cation, the experimental data indicate there are small or no barriers in excess of the endothermicities. The same complicated mechanistic possibilities mentioned above hold, and in addition, a pathway that involves the migration of two D atoms from the methane to separate iron atoms to form an $(FeD)(FeD)(FeCD_2)^+$ intermediate and possible bridging ligands might also be considered. Clearly, this type of intermediate is not possible for smaller clusters but is for all larger clusters. Now, dehydrogenation can occur remotely from the $Fe_n^+-CD_2$ bond, which may help to explain the disappearance of the barrier in the exit channel. Further, as the number of iron atoms increases, the electronic flexibility of the cluster is enhanced such that the barrier for D_2 elimination may be reduced.

According to this line of reasoning, clusters larger than the tetramer are also unlikely to have large barriers to D_2 elimination. This hypothesis is consistent with our assignment of the observed barriers to reaction (4), $\sim 0.70 \pm 0.30$ eV for $n>6$, to the initial C–D activation step. The observation of comparable thresholds for formation of the $Fe_nCD_4^+$ and $Fe_nCD_2^+$ products for $n=10-15$ is consistent with a common barrier for production of the $Fe_nCD_4^+$ intermediate, but inconsistent with a barrier lying in the exit channel for dehydrogenation.

VI. CONCLUSION

The kinetic energy dependences of the reactions of size-specific iron cluster cations ($n=2-15$) with deuterated methane are examined in a tandem guided ion beam mass spectrometer. We report cross sections for about 12 reactions for each cluster system ($Fe_n^+ + CD_4$), all of which exhibit thresholds. The main reactions observed are the dehydrogenation reactions (4), double dehydrogenation reactions (2), and reactions (1) to form $Fe_nCD_2^+$, Fe_nC^+, and Fe_nD^+, respectively. Analyses of the energy dependence of both primary and secondary routes to the various products provides two independent routes to bond energies for each cluster to D, C, CD, and CD_2. The two values are in good agreement except in the case of CD_2, which is evidence that there are barriers in excess of the endothermicity of the initial dehydrogenation reaction, except for $n=3$ and 4. These barriers for reaction of the monomer and probably the dimer cations are in the exit channel, whereas for larger clusters, evidence points to the initial dissociative chemisorption step.

Our best estimates for C, CD, CD_2, and CD_3 binding energies to cationic iron clusters are from reactions (2), (3), (9), and (10), respectively. The relative magnitudes in D, C, CD, CD_2, and CD_3 bond energies to the iron cluster cations are consistent with simple bond order considerations (single, triple, triple, double, and single bond orders). Comparison of these values to limited experimental information for binding of atoms to surfaces suggests that our experimental bond energies for larger clusters should provide reasonable estimates for heats of adsorption to surfaces. As no experimental information is available for molecular species binding to surfaces, the thermochemistry derived here for clusters bound to C, CD, and CD_2 (and CD_3 in analogy to D) provides some of the first experimental thermodynamic information on such molecular species. These values are in reasonable accord with estimates obtained for CD, CD_2 and CD_3 binding to Fe/W(110) surfaces using the BOC-MP method.[63]

ACKNOWLEDGMENT

This work is supported by the Chemical Sciences, Geosciences, and Biosciences Division, Office of Basic Energy Sciences, Office of Science, U.S. Department of Energy.

[1] G. P. Van der Laan and A. A. C. M. Beenackers, Ind. Eng. Chem. Res. **38**, 1277 (1999).
[2] J. R. Rostrup-Nielsen, in *Catalysis Science*, edited by J. R. Anderson and M. Boudart (Springer, Berlin, 1984), Vol. 5.
[3] H. Yang and J. L. Whitten, Surf. Sci. **289**, 30 (1993).
[4] A. N. Conejo and G. P. Martins, Ironmaking Steelmaking **26**, 111 (1999).
[5] O. Stelling, US Patent No. 2,780,537 (1957).
[6] P. R. Gray and B. J. Leroy, US Patent No. 3,885,023 (1975).
[7] F. M. Stephenes, US Patent No. 4,053,301 (1977); F. A. Stephenes, J. P. Hager, and F. M. Stephenes, US Patent No. 5,073,194 (1991).
[8] P. G. Wright, P. G. Ashmore, and C. Kemball, Trans. Faraday Soc. **54**, 1692 (1958).
[9] A. B. Anderson and J. J. Maloney, J. Phys. Chem. **92**, 809 (1988).
[10] A. B. Anderson, J. Am. Chem. Soc. **99**, 696 (1975).
[11] P. B. Armentrout and B. L. Kickel, in *Organometallic Ion Chemistry*, edited by B. S. Freiser (Kluwer, Dordrecht, 1996), pp. 1–45.
[12] P. B. Armentrout, Int. J. Mass. Spectrom. **200**, 219 (2000).
[13] J. Conceição, S. K. Loh, L. Lian, and P. B. Armentrout, J. Chem. Phys. **104**, 3976 (1996).
[14] J. B. Griffin and P. B. Armentrout, J. Chem. Phys. **106**, 4448 (1997).
[15] J. B. Griffin and P. B. Armentrout, J. Chem. Phys. **107**, 5345 (1997).
[16] J. B. Griffin and P. B. Armentrout, J. Chem. Phys. **108**, 8062 (1998).
[17] J. B. Griffin and P. B. Armentrout, J. Chem. Phys. **108**, 8075 (1998).
[18] J. Xu, M. T. Rodgers, J. B. Griffin, and P. B. Armentrout, J. Chem. Phys. **108**, 9339 (1998).
[19] J. Conceição, R. Liyanage, and P. B. Armentrout, Chem. Phys. **262**, 115 (2000).
[20] R. Liyanage, J. Conceição, and P. B. Armentrout, J. Chem. Phys. (submitted).
[21] S. K. Loh, D. A. Hales, L. Lian, and P. B. Armentrout, J. Chem. Phys. **90**, 5466 (1989).
[22] T. G. Deitz, M. A. Duncan, D. E. Powers, and R. E. Smalley, J. Chem. Phys. **74**, 6511 (1981).
[23] C.-X. Su and P. B. Armentrout, J. Chem. Phys. **99**, 6506 (1993).
[24] D. A. Hales, C.-X. Su, L. Lian, and P. B. Armentrout, J. Chem. Phys. **100**, 1049 (1994).
[25] L. Lian, C.-X. Su, and P. B. Armentrout, J. Chem. Phys. **97**, 4072 (1992).
[26] E. Teloy and D. Gerlich, Chem. Phys. **4**, 417 (1974), D. Gerlich, Adv. Chem. Phys. **82**, 1 (1992).
[27] N. R. Daly, Rev. Sci. Instrum. **31**, 264 (1959).
[28] K. M. Ervin and P. B. Armentrout, J. Chem. Phys. **83**, 166 (1985).
[29] See EPAPS Document No. E-JCPSA6-115-009144 for 30 figures and 14 tables. This document may be retrieved via the EPAPS homepage (http://www.aip.org/pubservs/epaps.html) or from ftp.aip.org in the directory /epaps/. See the EPAPS homepage for more information.
[30] R. H. Shultz, J. L. Elkind, and P. B. Armentrout, J. Am. Chem. Soc. **110**, 411 (1988).
[31] C. L. Haynes, Y.-M. Chen, and P. B. Armentrout, J. Phys. Chem. **100**, 111 (1996).
[32] M. F. Jarrold and J. E. Bower, J. Chem. Phys. **87**, 5728 (1987).
[33] K. M. Ervin and P. B. Armentrout, J. Chem. Phys. **83**, 166 (1984).
[34] R. G. Gilbert and S. C. Smith, *Theory of Unimolecular and Recombination Reactions* (Blackwell Scientific, Oxford, 1990).
[35] D. G. Truhlar, B. C. Garrett, and S. J. Klippenstein, J. Phys. Chem. **100**, 12771 (1996).
[36] K. A. Holbrook, M. J. Pilling, and S. H. Robertson, *Unimolecular Reactions*, 2nd ed. (Wiley, New York, 1996).
[37] M. T. Rodgers, K. M. Ervin, and P. B. Armentrout, J. Chem. Phys. **106**, 4499 (1997).
[38] S.-C. Chang, R. H. Hauge, Z. H. Kafafi, J. L. Margrave, and W. E. Billups, J. Am. Chem. Soc. **110**, 7975 (1988).

[39] H. Huber and G. Herzberg, *Constants of Diatomic Molecules* (Van Nostrand Reinhold, New York, 1979).
[40] M. E. Jacox, "Vibrational and electronic energy levels of polyatomic transient molecules," in *J. Phys. Chem. Ref. Data Monograph No. 3* (American Chemical Society and AIP, Woodbury, NY, 1994).
[41] J. W. Kauffman, R. H. Hauge, and J. L. Margrave, High. Temp. Sci. **17**, 237 (1984).
[42] C. L. Haynes, Y.-M. Chen, and P. B. Armentrout, J. Phys. Chem. **100**, 111 (1996).
[43] M. T. Rodgers and P. B. Armentrout, J. Chem. Phys. **109**, 1787 (1998).
[44] V. A. Spasov, T. H. Lee, J. P. Maberry, and K. M. Ervin, J. Chem. Phys. **110**, 5208 (1999).
[45] M. Castro and D. R. Salahub, Phys. Rev. B **49**, 11842 (1994).
[46] D. G. Musaev and K. Morokuma, J. Chem. Phys. **101**, 10697 (1994).
[47] This Fe–D bond energy has been adjusted from the Fe–H bond energy given in R. H. Schultz and P. B. Armentrout, J. Chem. Phys. **94**, 2262 (1991), using Fe–H and Fe–D vibrational frequencies of 1764 and 1259 cm^{-1}, respectively, taken from A. Dendramis, R. J. Van Zee, and W. Weltner, J. Astrophys. Astron. **231**, 632 (1979).
[48] P. B. Armentrout, ACS Symp. Ser. **428**, 18 (1990).
[49] Thermochemistry for deuterated fragments of CD_4 is compiled in Ref. 31.
[50] R. H. Schultz and P. B. Armentrout, Organometallics **11**, 828 (1992).
[51] P. Schnabel, M. P. Irion, and K. G. Weil, J. Phys. Chem. **95**, 9688 (1991).
[52] M. P. Irion and P. Schnabel, J. Phys. Chem. **95**, 10596 (1991).
[53] P. Schnabel and M. P. Irion, Ber. Bunsenges. Phys. Chem. **96**, 1101 (1992).
[54] T. Miller and B. Bederson, Adv. At. Mol. Phys. **13**, 1 (1977).
[55] K. J. Miller and J. A. Savchik, J. Am. Chem. Soc. **101**, 7206 (1979).
[56] M. L. Mandich, L. F. Halle, and J. L. Beauchamp, J. Am. Chem. Soc. **106**, 4403 (1984).
[57] J. L. Elkind and P. B. Armentrout, Inorg. Chem. **25**, 2765 (1986).
[58] J. L. Elkind and P. B. Armentrout, J. Phys. Chem. **91**, 2037 (1987).
[59] E. A. Carter and W. A. Goddard, III, J. Phys. Chem. **92**, 5679 (1988).
[60] P. B. Armentrout, L. S. Sunderlin, and E. R. Fisher, Inorg. Chem. **28**, 4437 (1989).
[61] M. R. Albert and J. T. Yates, Jr., *The Surface Scientist's Guide to Organometallic Chemistry* (American Chemical Society, Washington, DC, 1987).
[62] F. Boszo, G. Ertl, M. Grunze, and M. Weiss, Appl. Surf. Sci. **1**, 103 (1977); F. Bsozo, G. Ertl, and M. Weiss, J. Catal. **50**, 519 (1977).
[63] J. B. Benziger, in *Metal-Surface Reaction Energetics*, edited by E. Shustorovich (VCH, New York, 1991), p. 53.
[64] E. Shustorovich, Surf. Sci. Rep. **6**, 1 (1988).
[65] E. Shustorovich, Acc. Chem. Res. **21**, 183 (1988).
[66] E. Shustorovich, J. Mol. Catal. **54**, 301 (1989).
[67] E. Shustorovich, Adv. Catal. **37**, 101 (1990).
[68] A. T. Bell in Ref. 63, p. 191.